# Direct Ink Writing Using Agar-based Ink in 3D-printing of $Al_2O_3$ Membrane Support with Tubular Shape

**Kotchaphan Chaisong**

**A Thesis Submitted in Partial Fulfillment of the Requirements for the Degree of Master of Science in Materials Science**

**Prince of Songkla University**

**2023**

# Direct Ink Writing Using Agar-based Ink in 3D-printing of $Al_2O_3$ Membrane Support with Tubular Shape

**Kotchaphan Chaisong**

**A Thesis Submitted in Partial Fulfillment of the Requirements for the Degree of Master of Science in Materials Science**

**Prince of Songkla University**

**2023**

| | |
|---|---|
| **Thesis Title** | Direct Ink Writing Using Agar-based Ink in 3D-printing of $Al_2O_3$ Membrane Support with Tubular Shape |
| **Author** | Miss Kotchaphan Chaisong |
| **Major Program** | Materials Science |

---

**Major Advisor**

……..
(Asst. Prof. Dr. Kowit Lertwittayanon)

**Co-advisor**

……..
(Dr. Kanit Soongprasit)

**Examining Committee:**

……Chairperson
(Asst. Prof. Dr. Wichitpan Rongwong)

……..Committee
(Assoc. Prof. Dr. Anukorn Phuruangrat)

……..Committee
(Asst. Prof. Dr. Methee Promsawat)

……..Committee
(Asst. Prof. Dr. Kowit Lertwittayanon)

……..Committee
(Dr. Kanit Soongprasit)

The Graduate School, Prince of Songkla University, has approved this thesis as partial fulfillment of the requirements for the Master of Science, Degree in Materials science.

.....

(Asst. Prof. Dr. Thakerng Wongsirichot)
Acting Dean of Graduate School

This is to certify that the work here submitted is the result of the candidate's own investigations. Due acknowledgement has been made of any assistance received.

…….....…… Signature
(Asst. Prof. Dr. Kowit Lertwittayanon)
Major Advisor

….……..……Signature
(Dr. Kanit Soongprasit)
Co-advisor

….……..……Signature
(Miss Kotchaphan Chaisong)
Candidate

I hereby certify that this work has not been accepted in substance for any degree, and is not being currently submitted in candidature for any degree.

..…… Signature
(Miss Kotchaphan Chaisong)
Candidate

| | |
|---|---|
| **Thesis Title** | Direct ink writing using agar-based ink in 3D-printing of $Al_2O_3$ membrane support with tubular shape |
| **Author** | Kotchaphan Chaisong |
| **Major Program** | Materials Science |
| **Academic Year** | 2022 |

## ABSTRACT

The forming technique of tubular alumina membrane from agar by using 3D printing technology on direct inking technique is a process to reduce the cost and environmental friendliness. Alumina ceramic ink for 3D printing was prepared using TM-5D type of alumina powder with a particle size of 0.2 μm at a solid ratio of 80 wt%. The agar solution at concentrations of 1, 2, 3 and 4 wt% were analyzed the viscosity and gelation temperature were. Preliminary results show that 4 wt% concentration of agar solution is optimum for 3D printing. However, the further improvement of the rheological properties is required by adding 10 wt% of polyethylene glycol 1500 and hydroxyethylene cellulose (HEC) at 0, 1 and 2 wt% into agar solution. The results showed that 2 wt% of HEC-added in alumina slurry inks provided the appropriate viscosity for 3D printing with perfect filament. In addition, it was found that adding acetone at 0, 10 and 20 wt% were improved the ink rapidly dry after extrusion through the nozzle. After drying the specimens at room temperature for 24 hours and then sintering at 1350oC, it was found that the amount of acetone affecting the apparent density of the printed alumina membrane tubes was 3.82. 3.99 and 4.03 g/cm3 when 0, 10 and 20 wt% of acetone were added, respectively. This study indicated that agar-assisted alumina slurry inks had potential for 3D printing to use as a binder for forming the tubular alumina membranes with 3D printing technology. However, the research team plans to improve fidelity in the future.

**ชื่อวิทยานิพนธ์** การเขียนหมึกโดยตรงโดยใช้หมึกเอการ์ในการพิมพ์สามมิติของตัวรองรับเมมเบรนอะลูมินาแบบท่อกลวง

**ผู้เขียน** นางสาวกชพรรณ ไชยสง

**สาขาวิชา** วัสดุศาสตร์

**ปีการศึกษา** 2565

## บทคัดย่อ

เทคนิคการขึ้นรูปเมมเบรนอะลูมินาแบบท่อจากวัตถุดิบวุ้นเอการ์ด้วยเทคโนโลยีการพิมพ์สามมิติเทคนิคการเขียนหมึกโดยตรงนั้นเป็นกระบวนการที่สามารถลดต้นทุนด้านราคา และความเป็นมิตรต่อสิ่งแวดล้อม โดยทำการเตรียมหมึกพิมพ์เซรามิกอะลูมินาสเลอรี่สำหรับการพิมพ์สามมิติโดยการใช้ผงอะลูมินาชนิด TM-5D ขนาดอนุภาค 0.2 μm ที่สัดส่วนของแข็ง 80 wt% โดยสารละลายวุ้นเอการ์มีการเตรียมที่ความเข้มข้น 1 2 3 และ 4 wt% จากนั้นนำไปวิเคราะห์ความหนืดและอุณหภูมิในการเกิดเจล ผลการทดลองเบื้องต้นแสดงให้เห็นว่าที่ความเข้มข้นสารละลายวุ้นเอการ์ 4 wt% นั้นมีความเหมาะสมในการพิมพ์สามมิติมากที่สุดแต่ยังต้องมีการปรับปรุงสมบัติด้านการไหลต่อไป โดยการเติมโพลิเอทิลีนไกลคอล 1500 ปริมาณ 10 wt% และไฮดรอกซีเอทิลีนเซลลูโลส (HEC) ที่ 0 1 และ 2 wt% ลงในสารละลายวุ้นเอการ์ ผลการทดลองพบว่าหมึกพิมพ์เซรามิกอะลูมินาสเลอรี่ที่เติม HEC จำนวน 2 wt% ให้ความหนืดที่เหมาะสมต่อการพิมพ์สามมิติซึ่งให้เส้นฟิลาเมนต์ที่สมบูรณ์ นอกจากนี้พบว่าการเติมอะซิโตนที่ 0 10 และ 20 wt% ช่วยให้หมึกพิมพ์แห้งเร็วขึ้นภายหลังการรีดผ่านหัวฉีด โดยหลังปล่อยชิ้นงานให้แห้งที่อุณภูมิห้องเป็นเวลา 24 ชั่วโมงแล้วเผาผนึกที่ 1350°C พบว่าปริมาณอะซิโตนส่งผลต่อความหนาแน่นปรากฏของท่ออะลูมินาเมมเบรนที่พิมพ์ได้นั่นคือ 3.82 3.99 และ 4.03 g/cm$^3$ เมื่อมีการเติมอะซิโตน 0 10 และ 20 wt% ตามลำดับ การศึกษาในครั้งนี้ชี้ให้เห็นว่าหมึกพิมพ์เซรามิกอะลูมินาสเลอรี่ที่ใช้วุ้นเอการ์ช่วยในการพิมพ์สามมิติมีศักยภาพสำหรับการใช้เป็นตัวประสานสำหรับการขึ้นรูปเมมเบรนอะลูมินาแบบท่อด้วยเทคโนโลยีการพิมพ์สามมิติ อย่างไรก็ตามทีมวิจัยมีแผนในการปรับคุณสมบัติการรักษารูปร่างหลังการพิมพ์ (fidelity) ต่อไปในอนาคต

## ACKNOWLEDGMENTS

The research author would like to thank their deepest gratitude for the advice and instruction of all advisors under the supporting of Materials Science Program in Division of Physical Science, Center of Excellent in Membrane Science and Technology (CoE-MST) at Prince of Songkla University and the scholarship of Thailand Graduate Institute of Science and Technology (TGIST) (grantee code: TG-MT-PSU-63-057M). I would like to express my gratitude especially to Asst.Prof.Dr. Kowit Lertwittayanon who giving me a way and guideline to the goal achievement of the research work including to solve problem and all support, advice, and more opportunities for exchange opinions as myself thinking. Moreover, this thesis could not have done if without their helping and coorperation from co-advicesor Dr.Kanit Soongprasit. I would like to thank for learning experiences in the experimental laboratory at National Metal and Materials Technology Center (MTEC) including knowledge and useful advice on my research work. Additionally, I would like to thank Asst. Prof. Dr. Wichitpan Rongwong who kindly honored to be the chairpersonas as thesis examination, Assoc. Prof. Dr. Anukorn Phuruangrat and Asst. Prof. Dr. Methee Promsawat for your kindness as thesis examination committee and giving suggestions to the examination. Thank you to all person, friends, scientist in the Department of Materials Science and Technology helping in all assistance. Finally, I would like to thank my family for supporting understanding and encourage me during completing this thesis work.

Kotchaphan Chaisong

# CONTENTS

# CONTENTS (Continued)

# LIST OF TABLES

# LIST OF FIGURES

# LIST OF FIGURES (Continued)

# LIST OF FIGURES (Continued)

# LIST OF ABBREVIATIONS AND SYMBOLS

| Abbreviations and symbols | Full word and definition |
|---|---|
| $Al_2O_3$ | Alumina |
| HEC | Hydroxyethyl Cellulose |
| PEG1500 | Polyethylene Glycol 1500 |
| Dispex AA-4040 | Ammonium salt of polyacrylic acid |
| SEM | Scanning Electron Microscope |
| wt% | Percent of weight |
| vol% | Percent of volume |
| RO | Reverse osmosis |
| HDPE | High Density Polyethylene |
| °C/min | Celsius per minute |
| s | Second |
| min | Minute |
| µm | Micrometer |
| MPa | Mega Pascal |
| $g/cm^3$ | Density (grams per cubic centimeter) |

# CHAPTER 1

## 1. INTRODUCTION

### 1.1 Background and Rationale

In the past years, 3-D printing is a new technology growing up modernly which has advantages compared to traditional processes which have been used for a long-time during production. The 3D printing, also known as additive manufacturing (AM) has been developed as an alternative production by building parts layer-by-layer. There are several techniques of 3-D printing method such as Stereolithography (SLA), Selective Laser Sintering (SLS), Fused Deposition Modeling (FDM), Digital Light Process (DLP), Multi Jet Fusion (MJF), PolyJet, Direct Metal Laser Sintering (DMLS), Electron Beam Melting (EBM) [1]. SLA and FDM methods are most commonly used in many applications because their advantages in flexible design, fast and simple production, print on demand, strength and lightweight parts, minimum waste, inexpensive cost-effectiveness, and being environmentally friendly [2][3]. At present, tubular ceramic membranes are very popular in most manufacturing industries especially food, beverage, medical manufacturing and many others including waste water treatment.

Membrane materials are mostly made of polymer materials (plate type), metal, ceramic (hollow or tubular), zeolite, carbon and glass, but at the industrial level, tubular ceramic membrane has been widely applied. The advantages of the ceramic membrane compared to the polymer membrane include high mechanical strength, chemical and thermal stability, long working lifetime, corrosive and chemicals resistant, environmentally friendly, high porosity, and high flux [4][5][6][7].

All ceramic membranes presently used in Thailand are imported from overseas, resulting in high costs and limited shapes that do not meet specific requirements due to import restrictions [8]. Thus, the using of ceramic membrane in Thailand is still limited. Most manufacturers use extrusion process which is a die compression because it can be done relatively quickly and can control the desired size. The fabrication by extruder is also a continuous forming process. However, the extrusion has a limitation in forming

production, which are highly investment and sometimes must import from overseas that highly cost. Moreover, this method is expensive for machines and makes it possible only for industrial production. Therefore, creating a new knowledge base for small ceramic production, using lower capital, can be easy to manage and low production costs by using agar-based to enhance manufacturing capabilities of ceramic membrane in 3-D printing or additive manufacturing process provides easier access to technology for small and medium-sized enterprises. It could expand the range of tubular ceramic membrane applications to match the application and requirement as well.

For example, the ceramic membrane operating under pressure condition that requires high mechanical strength. In addition, pore size affects permeability. The alumina membrane support was fabricated by using direct ink writing seeing additive manufacturing (AM) technique. Agar-based ink was proposed to form shapes in 3D-printed extrusion. The AM technique is a process of creates three dimensional objects by depositing materials layer by layer with using computer aided design, or CAD, software and make objects from printing of 3D model [9][10][11]. A 3D-printer was required to form complex shapes. The small size alumina particles are needed for final required properties of ceramic membranes. Due to the sintering and de-binding creating void and pore, they affected density, shrinkage and strength.

This research was performed to adjust the alumina slurry as an ink paste for printing. The ink preparation of agar-based composition focused on binders adding. The viscoelastic and shape fidelity of ink paste was important which are the reason in this study. The viscoelastic of ink paste relates to elastic and viscous behavior to improve the preparation and provide the appropriate viscosity for 3D printing. The agar hydrogel properties, i.e. the rheological behavior and optimum viscosity were studied. After sintering, the 3D-printed samples were examined in terms of density, shrinkage, and microstructure. Storage modulus of ink was analyzed by Discovery Hybrid Rheometers (DHR).

## 1.2 Objectives

- To prepare the $Al_2O_3$ ink paste for forming the tubular ceramic membrane by direct ink writing (DIW) using agar-based ink.

- To find suitable binder for ceramic membrane forming using DIW method.

- To find suitable parameters of 3D-printer device for ceramic ink paste in printing of tubular ceramic membrane.

### 1.3 Scopes of research

- Preparation of agar-based ink to obtain suitable rheological properties

  - variation of agar solution concentration: 1, 2, 3, and 4wt%
  - variation of additive in binder system: hydroxyethyl cellulose (HEC) 0, 1, and 2wt%, acetone varying at 0, 10, and 20wt%, Polyethylene glycol 1500(PEG1500) constant at 10wt%

- 3D-printing of tubular ceramic membrane using DIW method

- Sintering of printed tubular ceramic membrane

- Characterization techniques were used to investigate the physical properties of ink paste and sintered ceramic membrane as the following:

  - Discovery hybrid rheometer (DHR) to test in 2 modes; In ramp mode for the viscosity test and oscillation mode for the storage modulus (G'). The analyzing temperature were performed in range of 80 and 20$^{o}$C.
  - Archimedes method to determine porosity and water adsorption.
  - Scanning Electron Microscopy (SEM) to observe microstructure or morphology of sintered ceramic membrane.
  - Linear shrinkage of printed ceramic membrane after drying and sintering.

### 1.4 Research goals

- To develop a technique for preparing ceramic filament to form tubular $Al_2O_3$ membrane support by DIW technique.

- To reduce the import of tubular membrane from abroad

- To adapt the agar-based ink for printing other ceramic materials such as zirconia, porcelain body, etc.

# CHAPTER 2

## 2. BACHGROUND AND LITERATURE REVIEWS

### 2.1 Background

The research development of ceramic filament production to form a ceramic membrane using AM technology was possible. The research team has plans for further development by studies to improve the properties of alumina filaments. Then, the tubular ceramic membrane was formed by fused deposition modeling (FDM) technique. Direct ink writing (DIW) using the same working as FDM technique which requires a suitable nozzle type for the $Al_2O_3$ ink paste printed to filament. The study results depend on physical and chemical properties and parameter printing such as designing shapes from sketch up program, printing temperature and printing rate. There might be influence the properties of tubular ceramic membrane, such as size, shape and green density. De-binding and sintering to increase the density and strength of the tubular ceramic membrane. A literature review of 3D printing found that background and literature reviews of printing technology using direct ink writing (DIW), which is very popular today due to its ease of printing and adjustable size include desire design. It is easy to operate manually and inexpensive.

### 2.2 Theory of 3D printer

3D printing is defined as a process of creating three-dimension objects based on slurry or ink extrusion. It is popularly known as also additive manufacturing (AM), and Direct Ink Writing (DIW), and other names includes; Robocasting, Direct-Write Assembly (DWA) or Microrobotic Deposition (μRD) which is less frequently in use. The additive manufacturing technique building up 3D parts layer by layer on process of deposition and solidification of print materials. The function of different types of 3D printers specific to the required application shown in **Fig.2.2.2** [12] [13] [14] [15] [16]. The concentrated slurry or colloidal suspensions of ceramic powders in water is required for the appropriate rheological behavior on 3D printing with slurry-based ink. The 3D model was created from a digital file of computer aid design (CAD) which rapid prototyping. The STL file is

importantly required in the system of 3D printing. One mainly factors of 3D model parts ability depend on shape and geometry from the CAD that design object for build platform. The 3D printing is a new technique with a variety of advantages that are superior to traditional manufacturing such as producing a complex shape, flexible design, light-weight parts, cost-effective, short production time, and less materials waste etc. [17] [18] [19]. The 3D printing technology is divided into seven main types; 1. Material extrusion 2. Vat polymerization 3. Powder bed fusion 4. Material jetting 5. Binder jetting 6. Directed energy deposition 7. Sheet lamination which are now widely used subtypes from the seven main types as mentioned includes Fused Deposition Modeling (FDM), Stereolithography (SLA) or Digital Light Processing (DLP), SLS, and more types were learned. The most commonly used 3D printing technology was fused deposition modeling (FDM)/fused filament fabrication (FFF) The reason why today FDM or FFF is the most popular 3D printing type is that because of appropriate for home use [20].

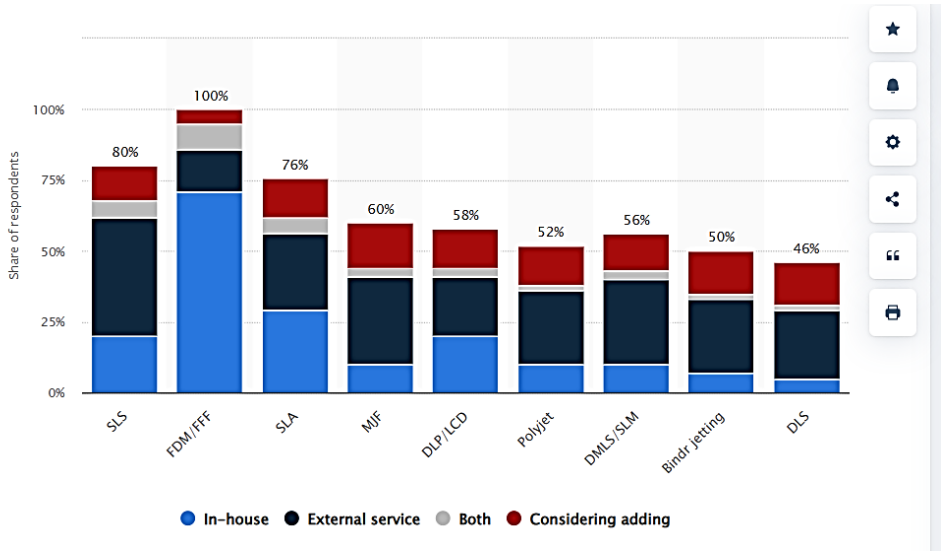


**Fig.2.2.1** The most used 3D printing technologies worldwide 2021 [20]

The types of 3D printing technology most used in 2022 are FDM (fused deposition modeling) as shown in **Fig.2.2.1** based on criteria of easily accessible to the normal population both cost and usage including benefit on people from 3D printing. However, fused deposition modeling or FDM technique is a technique that has been

continuously popular. The fused deposition modeling or FDM is a type of 3D printer for plastics forming by heated nozzle to melting materials. Melted plastic was extruded as a filament through nozzle deposited layer by layer on platform to build 3D shape [21][22] [23][24].

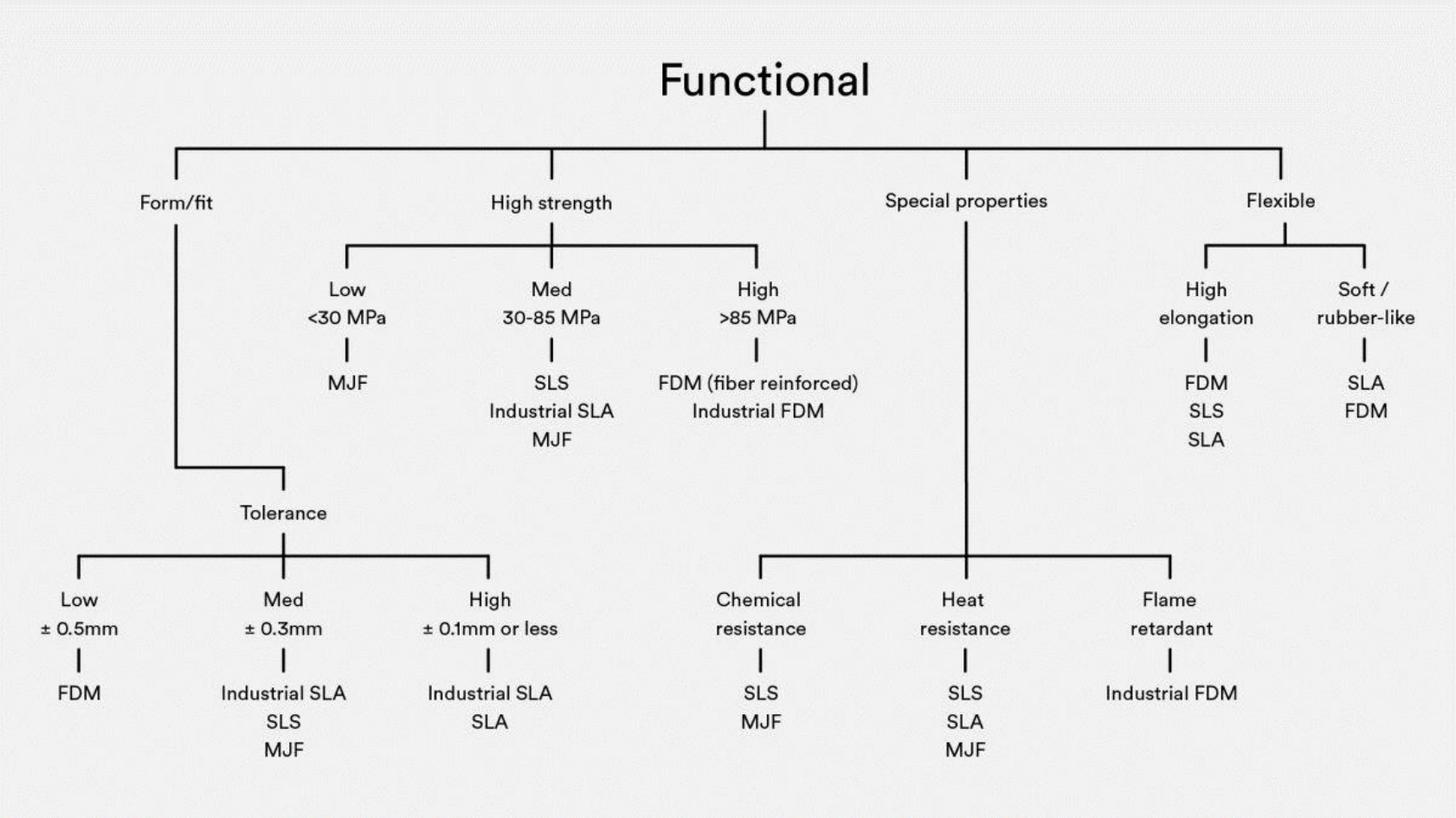


**Fig.2.2.2** The functional of different types of 3D printer [111]

Although the FDM technique same as direct ink writing (DIW) in working of extruding materials through nozzle. The distinct of FDM technique used polymer as a material to melt and able extrude through nozzle but DIW usually used ceramic slurry as ink for extruding through 3D printer nozzle and processing on a sintering to achieve mechanical strength. Therefore, DIW of 3D printing is necessary and suitable for use in ceramic printing [25].

## 2.3 Literature reviews

**In 2021, H. Xie et al.** [26] studied the 3D gel printing process of dense alumina ceramic by HEC addition applied in preparation of gel ink to adjust the rheology properties which suitable for 3D printing and printability of the rigid gel made from boehmite and using PEG as a liquid desiccant.

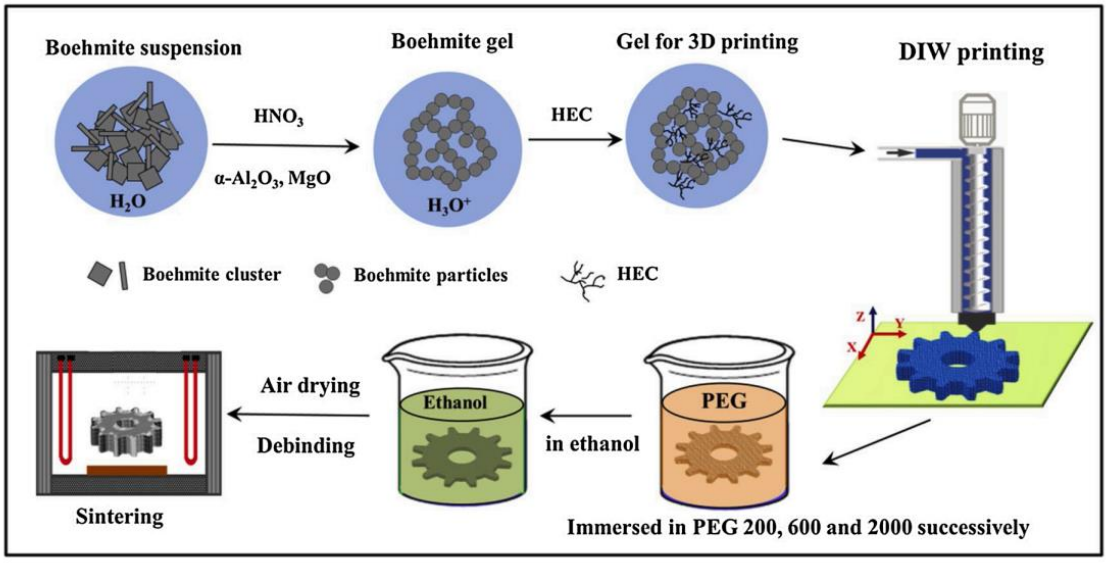


**Fig.2.3.1** Workflow of 3D gel printing followed by liquid desiccants drying and conventional pressure-less sintering

**Fig.2.3.1** shown workflow of 3D gel printing at the gel with 3wt%HEC and 30wt%boehmite affected on viscosity behavior as when take turn of shear rate. Reversible viscosity to prohibit the deformation. The gels containing 26, 30 and 34 wt% of boehmite influenced the storage modulus (G′) and loss modulus (G″) of the when shear stress

increases G′ falls whereas G″ rises until G′ = G″. At higher wt% boehmite receive higher G′ values and extend linear viscoelastic regions (LVR). However, decrease of G′ values given LVR about 100 Pa which might be not squeeze out in printing. Moreover, the storage modulus (G′) and loss modulus (G″) of the gels containing at higher HEC addition with 30wt%boehmite has no obvious effect on the maximum G′ value of 30wt%boehmite beneficial to extend the LVR to a certain degree. In printing gel at higher boehmite was affected on large drying or sintering shrinkage which approach to reduce the deforming or cracking relate that high solid content might be difficult in mixing, dispersion and gelation that the reason study at 30wt% boehmite.

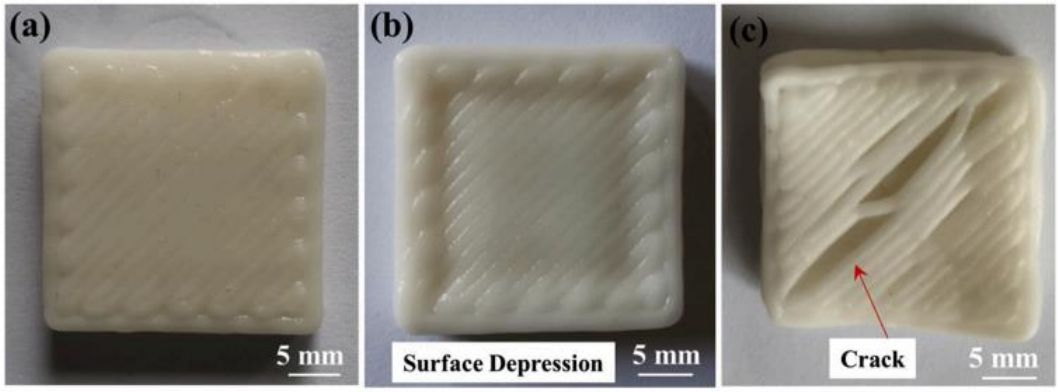


**Fig. 2.3.2** Photos of the dried samples: (a) without defects (b) surface depression (c) cracks along the printing path.

**Fig. 2.3.2** shown the surface depression and the cracks along the printing path are observing defects on the cuboid sample. Unavoidable defects in case of using PEG1000 or 2000 alone. When PEG 200 and 600 using, the linear shrinkage was observed at higher drying temperature and higher molecular weight of PEG. During the drying process, the liner shrinkage of green body reveals 21% of final body shrinkage and when alone using PEG200 cannot removed out of water and final linear shrinkage rise to 30% without defects by PEG with high molecular weight. The study of microstructure and the inter layer bonding related to the mechanical properties of alumina ceramics. The SEM images of dried surface and sintered body appeared the coherent interlayer bonding. Accordingly, layer thickness of the sintered body reduces to about 55 %. The relative

density of sintered alumina ceramics at 1450 $^{o}$C are 3.96 g/cm$^{3}$. alumina ceramics receive uniform, dense and fine grained about 1 μm

**In 2020, J. M. Habibur Rahmanthe et al.** [27] studied 3D food printing in terms of rheology and mechanical properties of agar and Konjac based edible gels in different ratios effects on the viscosity of the prepared food paste and the performance of 3D food printing gel with cold setting method. The procedure is dissolving the agar powder in distilled water and konjac powder with hot water. The agar solution and the konjac solution are mixed together, then varying weight ratio of agar powder and konjac powder Agar-konjac 3:1, Agar-Konjac 1:1 and Agar-konjac 1:3, respectively and prepared base of agar without konjac. The rheological test and compression test in food paste printing was heated at 100$^{o}$C to prevent gel formation and maintain proper viscosity. The result of the agar without konjac had the highest modulus from molecular aggregation to obtain rigid structure. As for agar: konjac ratio at 3:1, modulus decreased by more than 0.1% as strain increases, it affects the viscosity in forming the network structure.

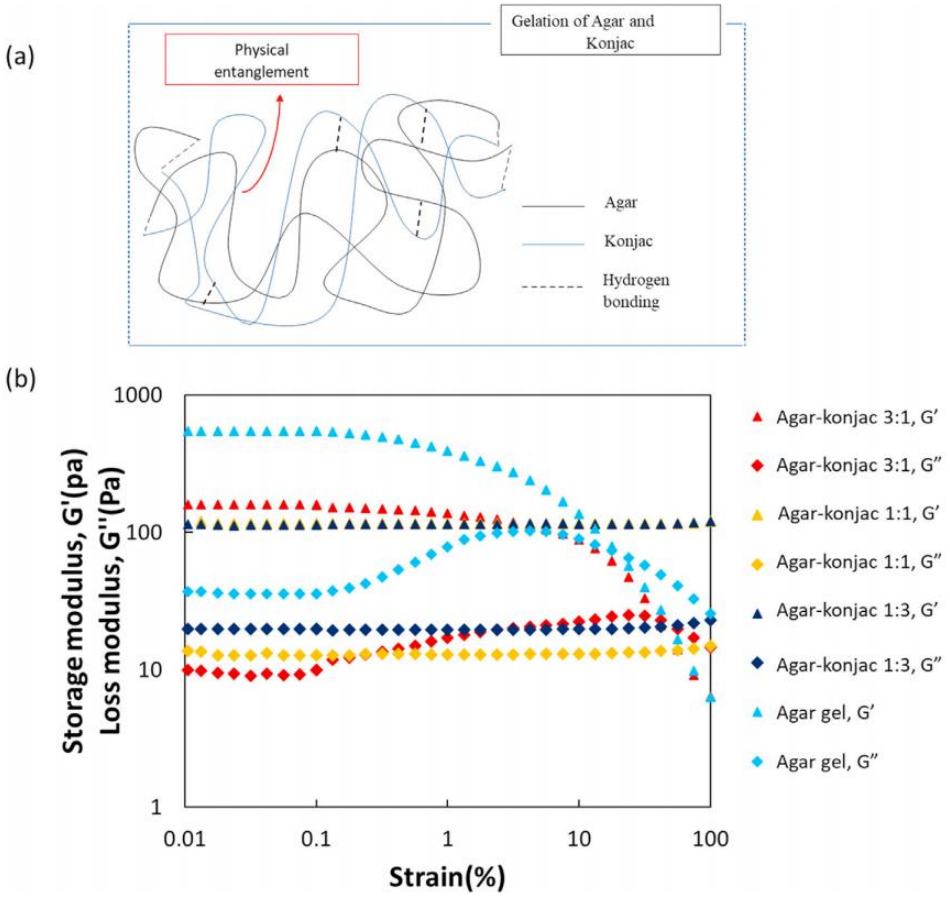


**Fig.2.3.3** (a) schematic illustration of gel network and b) strain- sweep analysis of the gel samples

Rheology study results: dynamic strain sweep analysis of gel by evaluating the viscosity properties. In **Fig. 2.3.3 (a)** shows the gel network, storage modulus and loss modulus curves of gel and **Fig. 2.3.3 (b)** Strain-sweep analysis of gel shows highest storage modulus (G') of agar without konjac because molecular aggregation strengthened the structure. For agar-konjac, the G' value decreased with increasing amount of konjac because the konjac molecules reduced the network of structure and lose rigidity due to increased stress from increasing konjac content, as in the case of agar-konjac 3:1

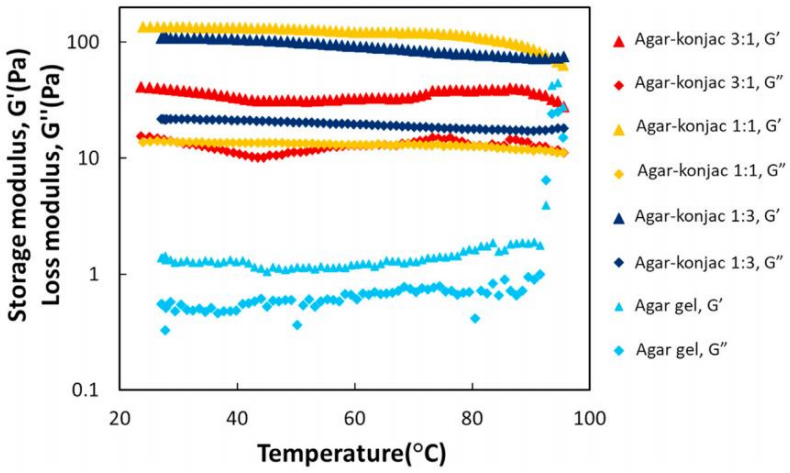


**Fig.2.3.4** Temperature-sweep analysis of the gel samples

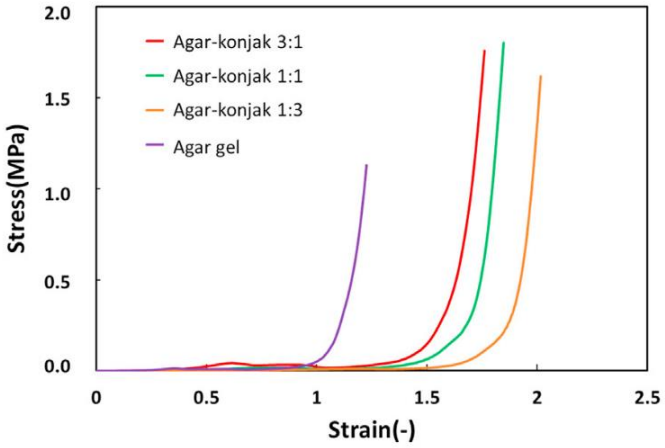


**Fig.2.3.5** Representative stress-strain curve for gel samples from compression test.

Rheology results: temperature sweep analysis in **Fig. 2.3.4,** agar-konjac at increasing temperature breaks down the molecular lattice to weakens network. The stress-strain curve is shown in **Fig. 2.3.5** agar without konjac had maximum stress and least elasticity. In contrary, when the amount of konjac increases, the modulus decreases that making the gel softer and ductile. The addition of konjac affects the network structure to be more flexible due to the adjustment of viscosity properties. Moreover, it has also been found that the addition of Konjac is useful for 3D printing smooth.

**In 2021, A. Paterlini et al.** [28] investigated the feasibility of generating 3D scaffold structures by robocasting 3 D printing for bone tissue engineering and anatomical model applications using additive manufacturing (AM) technology, 3 D printing by computer aided design (CAD) with self-setting pastes method based on deposited layer-by-layer through a syringe nozzle including considered in terms of manufacturing process and chemical setting reactions of ink paste to produce 3D scaffold structures. A self-setting reaction occurs from a calcium phosphate cement was used to form bone-like apatite scaffolds and hydrate calcium sulphate by self-setting reaction from calcium sulphate hemi-hydrate (bassanite) to calcium sulphate dihydrate (gypsum) and brushite powder and vaterite mixture to apatite by using a BCN3D printer with Fused Filament Fabrication (FFF) technique to inject a paste through the syringe nozzle. The investigation of this study is phase composition, rheology behavior of pastes, drying treatment and the testing of setting reactions, 3D samples characterization, water absorption test and compression test. Paste rheology behavior in terms of viscosity focus on printing flow. Moreover, water absorption test to assess the resistivity of the 3D sample which resulting 3D printing will not appear macro-porosity and also affects the mechanical properties of the samples. The self-setting reaction of calcium sulphate paste resulting in homogeneity and long setting time approach to occur hardening reaction. In analyzing the shear thinning behavior of calcium sulphate scaffolds suitable for bone models and additives addition improves the mechanical properties included different nozzles contribute to improving print resolution due to self-setting that can print biocompatible materials.

**In 2021, J. Wang et al.** [29] studied the rheological properties adjustment of inks for calcium alginate/agar (CA/Ag) 3D structure. The influent after printing is swelling behavior and mechanical properties on printing gels. The extrusion printing is an improving of FDM technology by extruding continuous liquid ink to obtain 3D printing structures with high precision. Three-dimensional structure of calcium alginate/agar (CA/Ag) was studied by adjusting the rheology of the printing ink by mixing alginate and agar to reduce the Barus effect by using agar to change the rheology properties of the ink by increasing the viscosity of ink. The viscosity occurs from swelling behavior of interface

layer adhesion after printing and mechanical properties received from printing resolution controlled by reducing the Barus effect due to viscosity.

Hydrogel 3D printing using a 2-steps method with cross-link structure or network hydrogel of prepared ink. The rheology result of ink reduced viscosity by increase sodium alginate (SA) resulting in poor formability of 3D printing but at higher viscosity was high surface tension which better forming. However, high viscosity of SA/Ag exhibited at low temperature due to the polymerization properties of agar which contributes to the mechanical properties from swelling and deswelling properties by cross-linking lead to high modulus and compressive strength. At increasing of SA content, the viscosity slightly decreased. The low viscosity unsuitable for 3D printing which SA added with agar (Ag) result to increase viscosity and high surface tension can help improve viscosity in the printing process. The rheology test at different temperatures found the viscosity increasing of mixing ink with decreasing temperature due to gelation of agar. As the SA content increases, the viscosity increases. This result to the ink filament to pass out larger than the diameter of nozzle.

**In 2021, C. Gadea et al.** [30] prepared the inks and the characteristics of reactive-colloidal hybrid ink for ceramic 3D printing or additive manufacturing (AM) technology. The robocasting technique to produce $BaTiO_3$-based electro-ceramics using hybrid inks of $BaTiO_3$-based ceramics for 3D printing layer-by-layer. The fuse deposition occurs when printing ink extruded through the nozzle. Colloids preparing (colloidal powder) and sol-gels (stabilized sol-gel suspension), also known as “hybrid sol-gel.”. The reaction between BaO and the Ti sol-gel solution results in deposition of $BaTiO_3$ 3D objects. In this work, the process of preparing inks suitable for use with robocasting or Direct ink writing (DIW) techniques by using of hybrid inks of $BaTiO_3$-based ceramics in 3D printing. To produces complex ceramics that are better than the traditional method based on the principle of fuse deposition of hybrid ink prepared from Titanium isopropoxide, 3 factors were prepared without glycerol, with glycerol and with glyceral+$BaTiO_3$ by injecting ink under controlled of air pressure onto a CAD-controlled printing substrate. The result of increase viscosity due to increase in shear stress. The addition of glycerol reduces

sedimentation, poor particle dispersion and makes the print shape relatively stable. The isopropoxide help to quickly reduce precipitation by adding Ti-based solvent-based glycol. The effect of glycerol precipitation on the flow behavior hindered by glycerol that showing shear thinning behavior not suitable for robocasting. As increase of solid loading influent on increase viscosity which affects the stress of parts and might be deform in 3D printing. The water-based hybrid inks from Ti-isopropoxide reaction and BaO, and $BaTiO_3$ colloidal from $BaTiO_3$ powder. The glycerol-added HI-$BaTiO_3$ sol gel inks to avoid rapid precipitation of $BaTiO_3$ sol. After sintering at $1350^oC$ obtained a density about 96% and demonstrates the robocasting application of hybrid ink to generate a complex shape of $BaTiO_3$-based electroceramics.

# CHAPTER 3

## 3. RESEARCH METHODOLOGY

### 3.1 Materials

$Al_2O_3$ powder (A-325, Claymin.co.th, Thailand) with an average particle size of 15-20 μm was used for a preliminary experiment in preparing $Al_2O_3$ ink paste. In addition, an α-$Al_2O_3$ powder (TM-5D, Taimei Co., Ltd., Japan) with an average particle size of 0.2 μm was employed for printing the tubular $Al_2O_3$ membrane support. Magnesium oxide (MgO) nano-powder (Alfa Aesar) was used as a sintering aid and also a inhibitor of abnormal grain growth. Ammonium salt of polyacrylate (Dispex AA-4040, BASF) was employed as a dispersant. Agar powder functioning as a gelling agent and a thickener was added to the ink paste in the form of agar solution. Hydroxyethyl cellulose (HEC, Ashland Industries, Netherlands) was also used as the thickener and a stabilizer to increase the viscosity of the ink paste. Polyethylene glycol 1500 (PEG 1500, Loba Chemie PVT. Ltd) was used as a lubricant. Acetone (99.8% purity) was added to the prepared ink paste to allow the extrude ink paste dry faster. Reverse osmosis (R/O) water was used in the preparation of all printing ink.

### 3.2 Ink preparation

#### 3.2.1 Preliminary ink preparation

**Part I:** The $Al_2O_3$ slurry having 80wt% solid loading was prepared from $Al_2O_3$ powder (A-325). MgO and Dispex AA-4040 (dispersant) were added at 0.03wt% and 1wt% of solid loading, respectively. Dispex AA-4040 was dissolved in RO water before mixing with the other substances in HDPE bottle using $Al_2O_3$ beads for dispersing all the substances. The ball milling was performed for 2 h. After ball milling, the prepared $Al_2O_3$ slurry was weighted and then kept warm in an ultrasonic bath at 60$^{o}$C

**Part II:** $Al_2O_3$ slurry weight has been calculated to prepare agar solution by mixing of agar powder and RO water. Final agar fixed at 2wt%. Agar solution was prepared at difference concentration of 1, 2, 3, and 4wt% to compare and select rheological behaviors suitable for using as the printing ink paste. Agar powder at the different concentrations was boiled at ~150 $^oC$ in a glass beaker put on a hotplate until a yellow solution was obtained. In the boiling, a magnetic bar stirrer was used to completely dissolve the agar powder. Due to the boiling, the evaporation of water occurred, the boiling was conducted in a closed system to prevent the water evaporation by covering the beaker with aluminum foil.

### 3.2.2 Mixing step for ink paste preparation

After the rheological analysis of agar solution with the different concentrations, one of the ink mixtures was carefully selected and improved further by adding additives and reducing the amount of liquid in the mixture.

The preparation of ink paste followed the part I of 3.2.1 but changed from the alumina powder A-325 to TM-5D. In part II of 3.2.1, the different concentrations of agar solution were examined to find an optimum viscosity of ink paste. The proper agar solution concentration at 4wt% of solid loading was selected. For water reducing, all substances in agar solution at 4wt% were calculated reducing by 50% of liquid loading. Agar powder and RO water were boiled to obtain 4wt% agar solution. Acetone was added into the agar solution at the amount using calculation at 10wt% of total agar solution weight. Two additives i.e. 2wt%HEC and 10wt%PEG1500 were calculated, and based on the loading of agar powder and then added into the clear agar solution, respectively. All substances were mixed by mechanical stirring at 150$^oC$ until homogeneity was observed. The flow chart of $Al_2O_3$ ink paste preparation for printing tubular membrane support by Eazao 3D-printer, China, was shown in Fig.3.1. Table.3.1 and 3.2 showed the composition of $Al_2O_3$ slurry and proportion of raw materials prepared %additive adding by section of nomenclatures A and B, respectively.

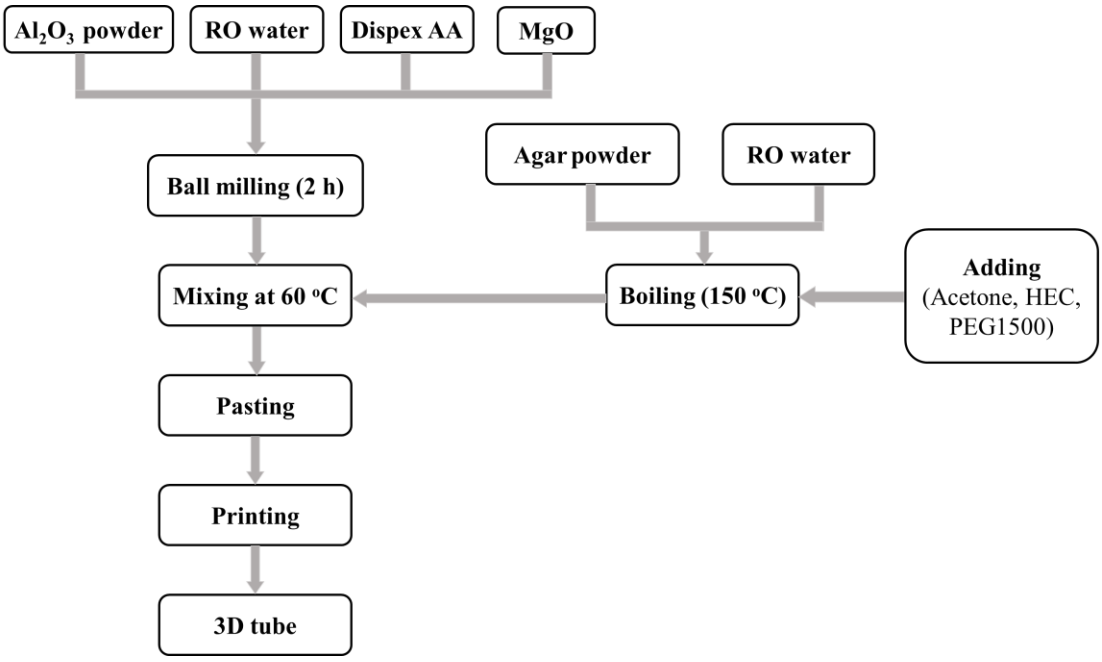


**Fig.3.1** Flow chart of $Al_2O_3$ ink paste preparation for printing tubular membrane support by Eazao 3D-printer

**Table.3.1A** Composition of $Al_2O_3$ slurry

| 80wt% $Al_2O_3$ | 20wt% $H_2O$ | 0.03wt% MgO | 1wt% DispexAA-4040 |
|---|---|---|---|
| 80 g. | 20 g. | 0.024 g. | 0.8 g. |

**Table.3.1B** 100 g. of $Al_2O_3$ slurry after ball milling for agar mixture preparation

| Final agar (wt%) | Concentration of agar solution (wt%) | Agar powder (g) | $H_2O$ (g) |
|---|---|---|---|
| **2** | 1 | 1.6 | 153.6 |
| | 2 | 1.6 | 76.8 |
| | 3 | 1.6 | 51.2 |
| | 4 | 1.6 | 38.4 |

**Table.3.2A** True solid loading of $Al_2O_3$ slurry mixture

| Nomenclature | Concentration of agar solution (wt%) | Final agar content (wt%) | Final $Al_2O_3$ content (%) | $H_2O$ (%) |
|---|---|---|---|---|
| **A1** | 1 | 2 | 31.345 | 7.84 |
| **A2** | 2 | 2 | 44.84 | 11.21 |
| **A3** | 3 | 2 | 52.35 | 13.09 |
| **A4** | 4 | 2 | 57.14 | 14.29 |

**Table.3.2B** Ratio of ink paste composition

| Nomenclature | Concentration of agar solution (wt%) | Final agar content (wt%) | Acetone (wt%) | HEC (wt%) | PEG1500 (wt%) | Final $Al_2O_3$ content (%) | $H_2O$ (%) |
|---|---|---|---|---|---|---|---|
| B1 | 4 | 2 | 0 | **0** | 10 | 54.05 | 13.51 |
| B2 | 4 | 2 | 0 | **1** | 10 | 53.76 | 13.44 |
| B3 | 4 | 2 | 0 | **2** | 10 | 53.48 | 13.37 |
| B4 | 4 | 2 | **10** | 2 | 10 | 51.73 | 12.93 |
| B5 | 4 | 2 | **20** | 2 | 10 | 50.09 | 12.52 |

In addition, because of a lot of water content in the mixture based on slurry composition, reducing liquid content in the prepared mixture by 50% of water in agar solution.

## 3.3 3-D printing of tubular $Al_2O_3$ membrane

### 3.3.1 Designing 3-D model of membrane with tubular shape

Tubular $Al_2O_3$ membrane samples were fabricated by 3D printing based on an additive manufacturing technique. The tubular model was designed by a 3D model or STL file of the sketch-up program converting to G-code file. The sketch-up program was used to design, draft and sketch the desire model. The designed 3D model was

exported and save as the STL or obj file. After that Cura software of the Eazao 3D printer was set up on the computer and put the data of, extruder, and materials. Parameter setting of printing related to ink paste such as step-up of the nozzle on the Z axis, travel speed, print speed, infill speed, and thickness layer was filled in. Finally, slice preview, ink paste content and working time of printing were shown on the computer. The tubular shape was shown in Fig.3.2. The model was saved into SD card as a G-code file for printing on the Eazao 3D-printer.

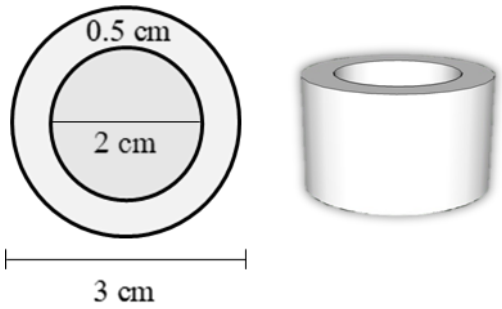


**Fig.3.2** Design of tubular shape from sketch-up program

**Table.3.3 Show the designed size of tubular shape.**

| ***Tubular shape*** | ***Size*** |
|---|---|
| *outer diameter* | 3 cm. |
| *inner diameter* | 2 cm. |
| *wall thickness* | 0.5 mm. |
| *height* | 2.5 cm. |

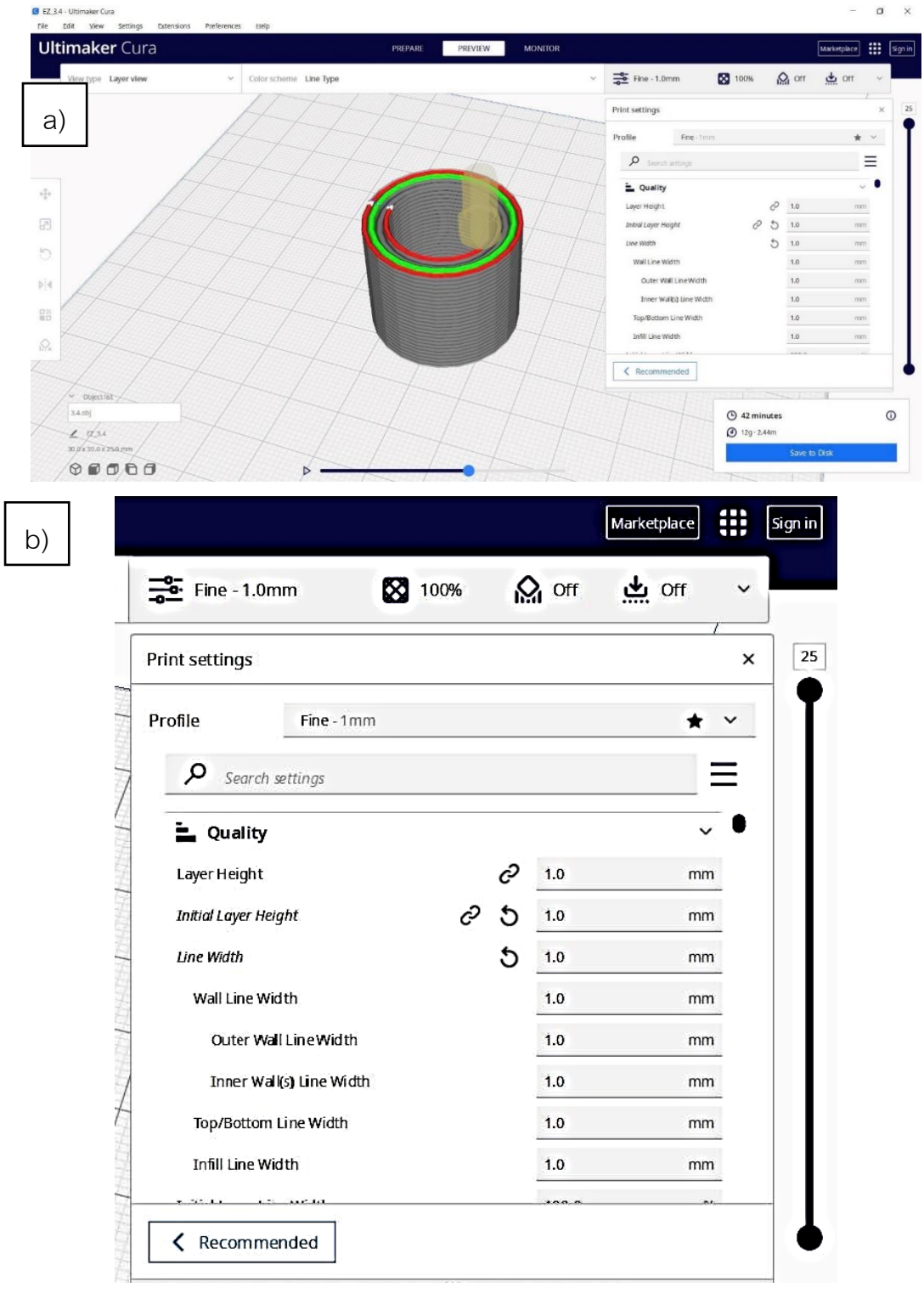


**Fig.3.3** Cura software of Eazao 3D-printer a) print preview and b) parameter setting

### 3.3.2 3D-printing

The prepared ink paste were printed using the Eazao 3-D printer. The Eazao 3D printer equipped with a syringe barrel to load the ink paste. The syringe barrel and extruder were the parts of printer that press and more the ink paste passing through a nozzle with 1.5 mm diameter. The schematic diagram illustrating the Eazao 3D-printer component was shown in **Fig.3.4**

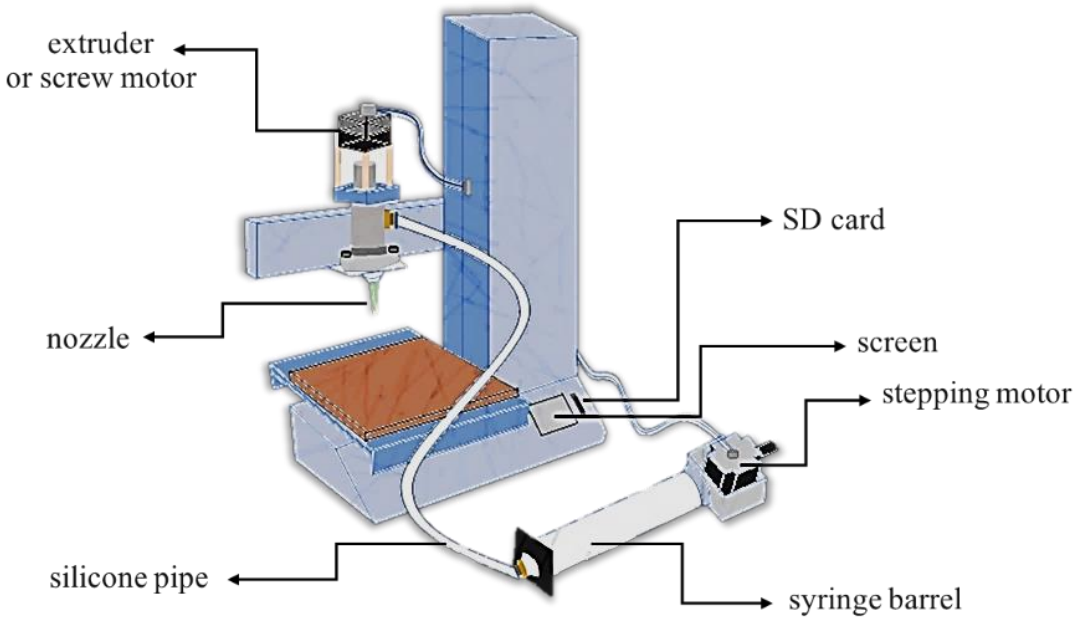


**Fig.3.4** Components of Eazao 3D-printer

## 3.4 Drying and sintering of green body

After printing, the samples were kept drying in air for 24 h to obtain green samples. Subsequently, all the samples were dried at 110 $^{o}$C to ensure that they were dried completed. The dried samples were sintered at 1300 $^{o}$C with heating rate at 5 $^{o}$C/min and holding time of 1 h. Finally, shrinkage of samples was recorded and calculated as the %firing shrinkage (%FS). The sintering step profile was shown in **Fig.3.5**

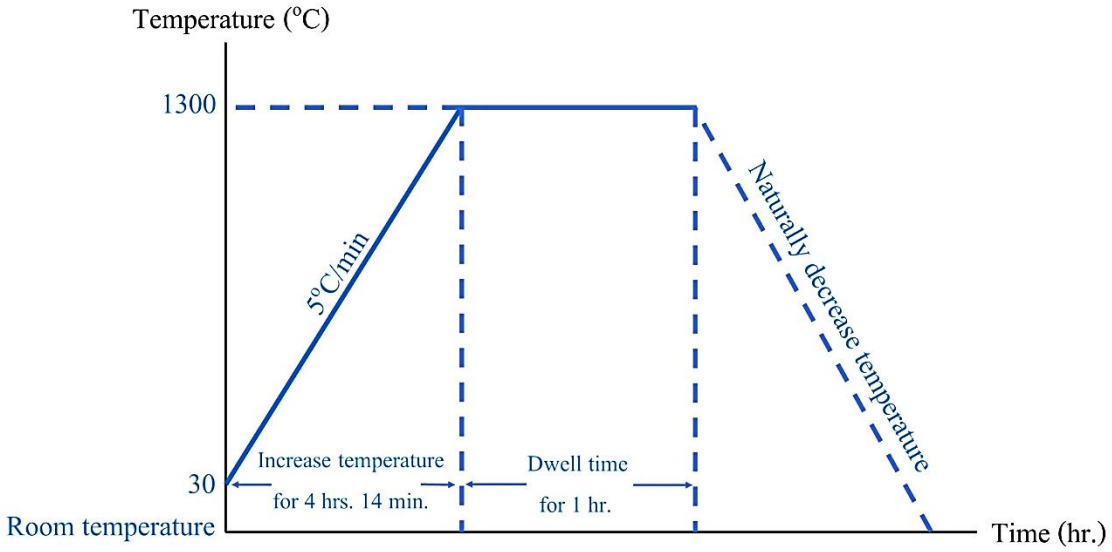


**Fig.3.5** Time-temperature profile of sintering the tubular $Al_2O_3$ membrane support.

$$\text{Time-temperature} = \frac{\text{temp.}_f - \text{temp.}_i}{\text{heating rate}} = \frac{1300-30\ ℃}{5\ ℃/\text{min}} = 254 \text{ min.} = 4 \text{ h.} 14 \text{ min.}$$

## 3.5 Characterization

### 3.5.1 Rheological analysis

To ensure that the ink paste was suitably extruded for the ink extrusion test at different concentrations of agar solution through the nozzle, gelling temperature must be known. The experiment on the rheological behavior was able to reveal glass transition temperature ($T_g$) and viscosity of printing ink for example, storage modulus, loss modulus, phase angle, and viscosity by using of discovery hybrid rheometer (DHR) with decreasing temperature from 80°C to 20°C. Subsequently, the optimal concentration was selected from the rheological analyzing of agar solution concentration varying at 1, 2, 3, and 4wt%.

### 3.5.2 Archimedes' method

The $Al_2O_3$ membrane relies on properties of porosity that refer to the ability of apparent porosity, water absorption, apparent density, and bulk density. The sample's weight after sintering was recorded. Fired weight, suspended weight, and saturated weight was calculated following Archimedes' method according to the American Society for Testing and Materials (ASTM) of designation: C 373 – 88.

The apparent density or $\rho_A$ of samples calculated by fired weight and suspended weight that conclude bulk volume and close porosity as follows the equation (1):

$$\rho_A = \frac{w_1}{w_1 - w_2} \quad (1)$$

Where; $w_1$ = fired weight

$w_2$ = suspended weight

The bulk density or $\rho_B$ is an exterior volume, close and open porosity and other defects of samples as follows the equation (2):

$$\rho_B = \frac{w_1}{w_3 - w_2} \quad (2)$$

Apparent porosity or $\%P_A$ is the total porosity in samples that can be replaced by water or also called open porosity follows by equations —(3):

$$\%P_A = \frac{w_3 - w_1}{w_3 - w_2} \times 100 = \frac{V_{op}}{V} \times 100 \quad (3)$$

Where; $w_3$ = saturated weight

The water absorption or $\%A_W$ is a water absorbed percentage of the dry samples which can calculate by weight of dry samples as follow the equations —(4):

$$\%A_W = \frac{w_3 - w_1}{w_1} \times 100 = \frac{V_{op}}{w_1} \times 100 \quad (4)$$

### 3.5.3 Determination of the linear shrinkage

The shrinkage of samples appeared after sintering which determine in terms of linear shrinkage.

Firing shrinkage or %FS is a measuring of length both height and width that was expressed as a relationship percentage. %FS calculation follows the equation (5):

$$\%FS = \frac{L_1 - L_2}{L_1} \times 100 \quad (5)$$

Where %FS is an average shrinkage after firing, $L_1$ is the length of the sample before firing and $L_2$ is the length of the sample after firing. The shrinkage calculation in both height and width uses the same equation.

### 3.5.4 Microstructure by scanning electron microscopy (SEM)

The printed samples are observed for the microstructure by scanning electron microscopy; SEM (JSM 5800LV, JEOL, Netherlands) at 20 kV. To analyze the cross-section image of samples, the sample surface must be conductive by gold sputtering technique before analysis for the electron beam interacts with atoms of samples and create the SEM images. The scanning electron microscope works by an electron source emitted an electron beam to impact the surface of the samples. The raster scan pattern of electron beam was scanned around the surface of the sample. Then the signals showed the topography details with other compositions of the surface on the computer.

For SEM analysis, the samples preparation was conducted from a small specimen fitted on stubs and the specimen have electrical conductivity by gold sputtering as mention before which suitable for using under condition of high vacuum system and high energy of electron beam.

# CHAPTER 4

## 4. RESULTS AND DISCUSSION

### 4.1 Preliminary result of ink paste

The preliminary ink fixed at 2wt% of final agar content with varying concentrations of agar solution at 1, 2, 3, and 4wt% was added into the $Al_2O_3$ slurry containing 80wt% solid loading. All ink mixtures were gelled during laying up by agar properties which an agar powder is one of compositions in the mixtures aiming to develop the mixture printing. Agar was selected in the ink preparation because agar was a type of hydrocolloid having specific properties for improving the viscosity during extrusion and the shape fidelity over the up-layering [31]. The preliminary experiment was to find the suitable proportion that the ink can be extruded with high solid loading.

At a condition of preparation, i.e., mechanical grinding by ball milling, mixing substances in HDPE bottle composing of 80wt%$Al_2O_3$ powder, 0.3wt%MgO, and 20wt%RO water, the surface of $Al_2O_3$ particles had a weak positive charge [32] which poorly dispersed or undispersed in ball milling resulting in the flocculation. De-flocculation by 1wt%dispex AA-4040 adding which act as a dispersant indicated that the polymer chain of dispex AA-4040 (Ammonium salt of polyacrylic acid) facing neutral side to weak positive charge on $Al_2O_3$ surface and exert a repulsive force by positive charge head or $NH_4^+$ of dispex AA-4040 (Ammonium salt of polyacrylic acid) to weak positive charge on $Al_2O_3$ surface which help to ensure the $Al_2O_3$ particles was completely dispersed [33][34][35][36][37]. Total charge resulting is a strong and long-ranged electrosteric repulsion. The achievement of dispersing alumina by poly-acids due to polymers ability created the electrical double layer (EDL) and steric repulsion [37]. The dispersion of electrosteric repulsion between $Al_2O_3$ particles and ammonium salt of polyacrylic acid shows in **Fig.4.1.1** Moreover, the addition of MgO help to decrease the sintering temperature because MgO act as a sintering aid and increase strength between particles. At

sintering temperature with MgO adding there was higher shrinkage and more densification by MgO added leading to improving mechanical properties [38][39]. Additionally, MgO did not affect or interact with other substance because MgO was neutral or zero charged. After the ball milling, the $Al_2O_3$ beads were removed from HDPE bottle and weighed only $Al_2O_3$ slurry before keeping warm in an ultrasonic bath at 60°C. This temperature was above the gelling temperature of agar solution used in mixing with $Al_2O_3$ slurry afterward.

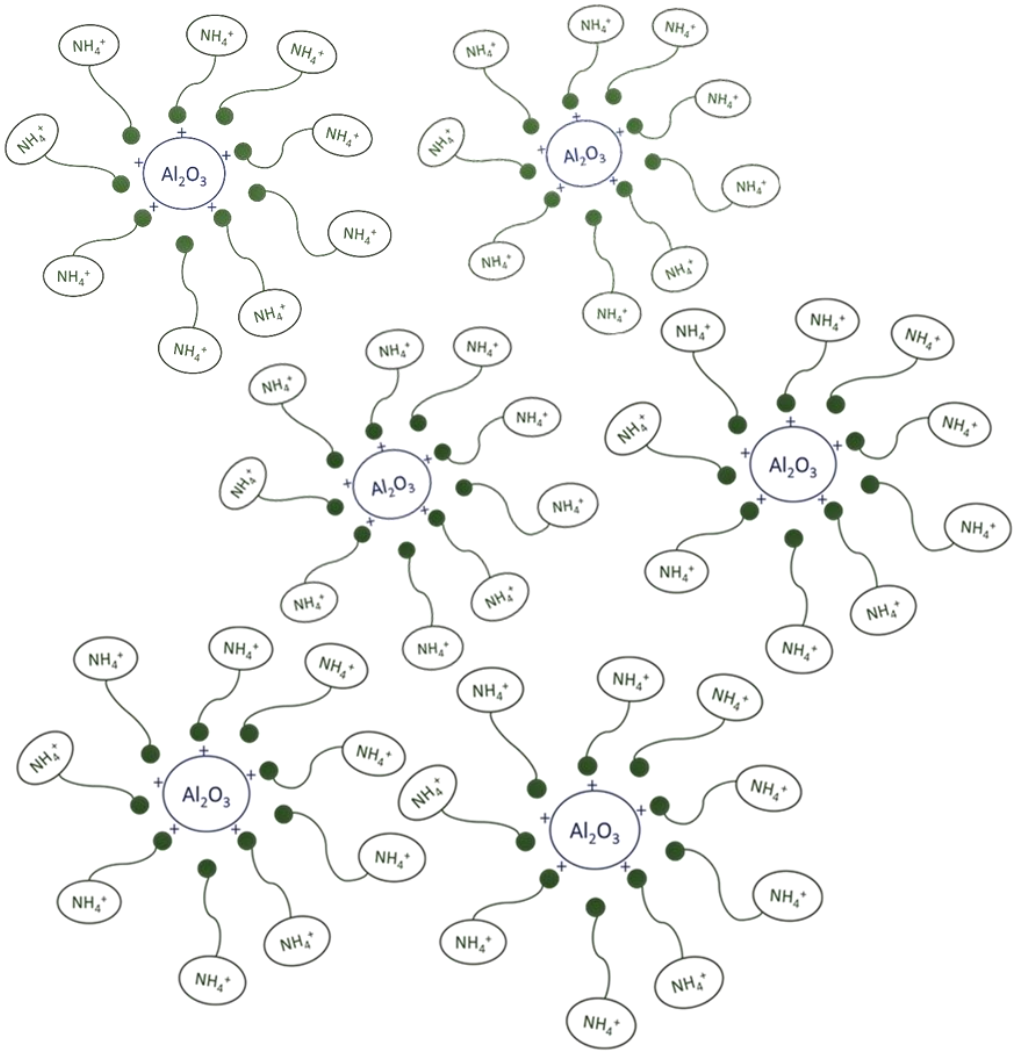


**Fig.4.1.1** The dispersion of electrosteric repulsion between $Al_2O_3$ particles and ammonium salt of polyacrylic acid

In preparation step of agar solution, after calculating the ratio of agar powder to water in boiling, agar powder along with RO water was boiled in a glass beaker put on a hotplate by using a magnetic stirrer to help rapidly and completely dissolve until the yellow clear solution was obtained. As boiling, agar solution might be evaporated at boiling point of water, closed system was essentials to use for this process to avoid and prevent the evaporation by covering it with aluminum foil.

The preliminary ink at 1, 2, 3, and 4wt% concentration of agar solution after extruding was observed. The results indicated that all the concentrations of agar solution in the inks mixture can extrude through 0.9 mm nozzle diameter. After extruding out for a few second, the gel formation of ink filament occurred due to the interaction of agar chains. It meant that there was cross link of the long polymer chains to produce a complex structure which was stronger. It was found that alginate, pectin, carrageenan, gelatin, gellan and agar normally were used for gelling [31]. Agar is one of hydrocolloid in carbohydrate types. Two polysaccharide combination in agar: agarose and agaropectin was attributed as an agar molecule. The chemical bonding between D-galactose and L-galactose in agarose bonding which are an agarobiose by glycosidic linkage at the end of structure as a long chain polymer. Agaropectin was more complex of the chemical structure than the agarose due to the sulfate group adhered in D-galactose and L-galactose. The high strength gelling property was given by the agarose component whereas the viscous properties was given by agaropectin [40]. The chemical structure of agar was shown in **Fig.4.1.2 [**41] Hydrocolloid is commonly used as gelling agent, thickening agent, stabilizing agent, emulsifier, fat replacer, flavor encapsulation [42] because its ability to thicken and gel it was the reason why agar was chosen for improving the ink rheology.

Therefore, a higher concentration of agar solution meant that a large amount of agarose and agaropectin are in the agar molecule. There was more interaction together in the helix structure or double helix generating the network structure stronger when the amount of agar increased [43].

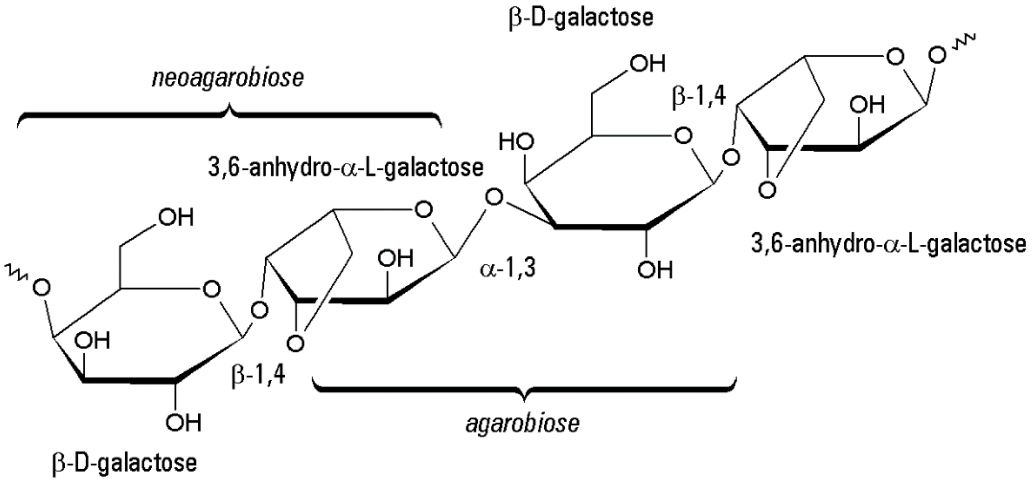


**Fig.4.1.2** The chemical structure of agar

Agar content in the prepared mixtures affected the property of ink. The printability of ink related to the viscosity of ink. The higher the agar content, the higher the viscosity. Thus, the importance of improving the $Al_2O_3$ ink mixture was the concentration of agar solution in the ink mixture. However, according to the agar properties forming a gel still occurred at below melting temperature of about 32 and 40°C [44]. when agar powder dissolves as a solution at a different concentration then cools it down, the gel formation is also formed at a different temperature [45].

Concentration at 4wt% of agar solution was selected because the experiment was required a high viscosity for layer-up and form shape which selected from the highest solubility of agar content [46]. Further study about gelling temperature, the tests were performed with syringe injection by the experimenter at various temperatures in the experiment as show in **Table.4.1**

**Table.4.1** $Al_2O_3$ ink paste with 4wt% concentration of agar solution by syringe of experimenter-controlled injection pressure at temperature from 43 decrease to 36ºC

| Temperature (ºC) | Top view | Side view |
|---|---|---|
| **43 ºC** |  |  |
| **42 ºC** | 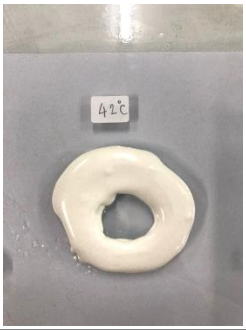 |  |
| **41 ºC** |  |  |
| **40 ºC** |  | 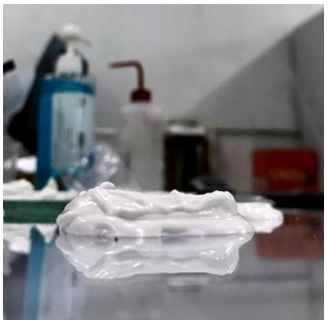 |

| Temperature (ºC) | Top view | Side view |
|---|---|---|
| **39 ºC** |  | 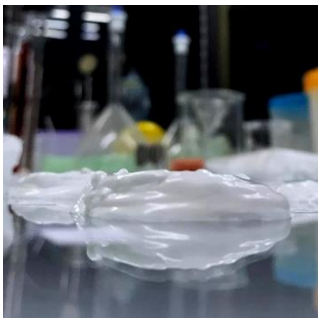 |
| **38 ºC** |  | 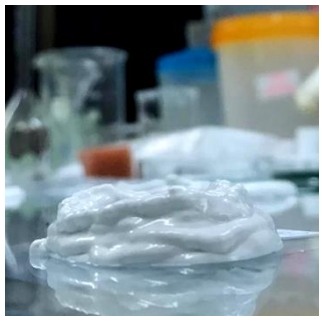 |
| **37 ºC** |  |  |
| **36 ºC** |  | 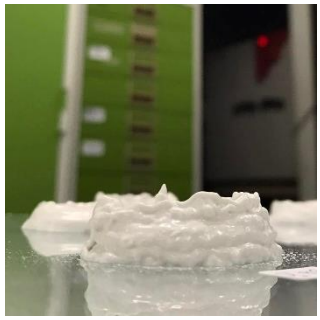 |

## 4.2 Rheological analysis

Agar was a gelling agent that could be dissolved in boiling water at higher 85$^{o}$C, and 1.5% agar gel formed at room temperature or about 32$^{o}$C-45$^{o}$C [45]. However, the gelling temperature depend on the concentration percent of the agar solution. The prepared ink from agar solution varied concentration at 1, 2, 3, and 4wt% without any additive adding was studied for rheology. All ink mixtures were analyzed by rheometer, which shows the degree of storage modulus, loss modulus, phase angle, and viscosity as shown in **Fig.4.2.1**

The optimal concentration of agar-based ink mixtures was selected from varying at 1, 2, 3, and 4wt% concentration of agar solution. The transition of gel state using discovery hybrid rheometer (DHR) to test in 2 modes; in ramp mode for testing the viscosity at shear rates of 1-100 $s^{-1}$ and in oscillation mode for measuring the storage modulus (G') at 1 Hz of frequency and ramp of 0.5$^{o}$C/s with the diameter of the measuring cup at 15 mm and the test gap at 1000 µm. The analyzing temperature were decreased in range of 80 to 20$^{o}$C.

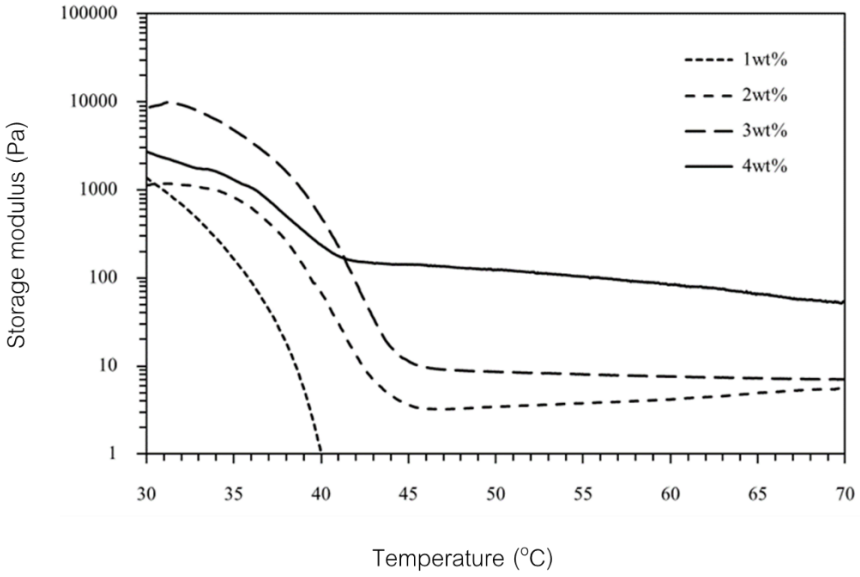


**Fig.4.2.1** Storage modulus of ink prepared from different concentration of agar solution at 1, 2, 3 and 4wt%

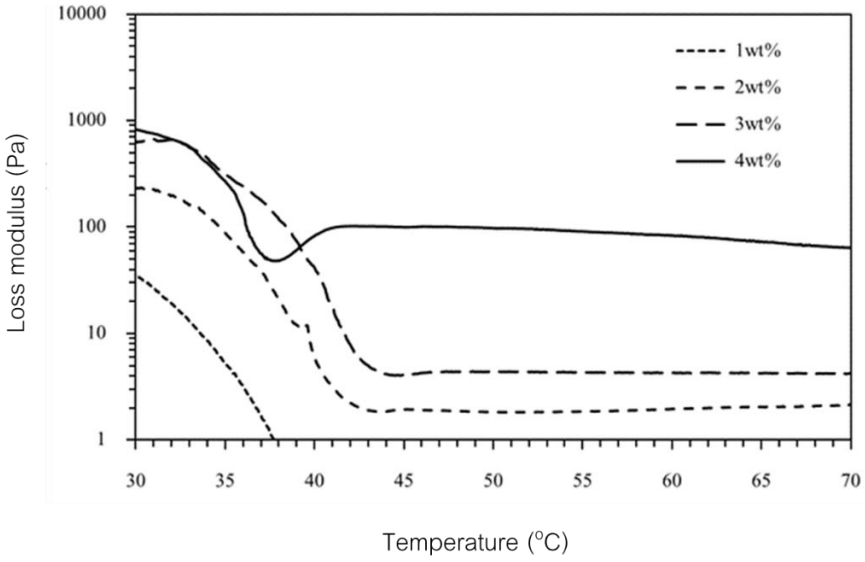


**Fig.4.2.2** Loss modulus of ink prepared from different concentration of agar solution at 1, 2, 3 and 4wt%

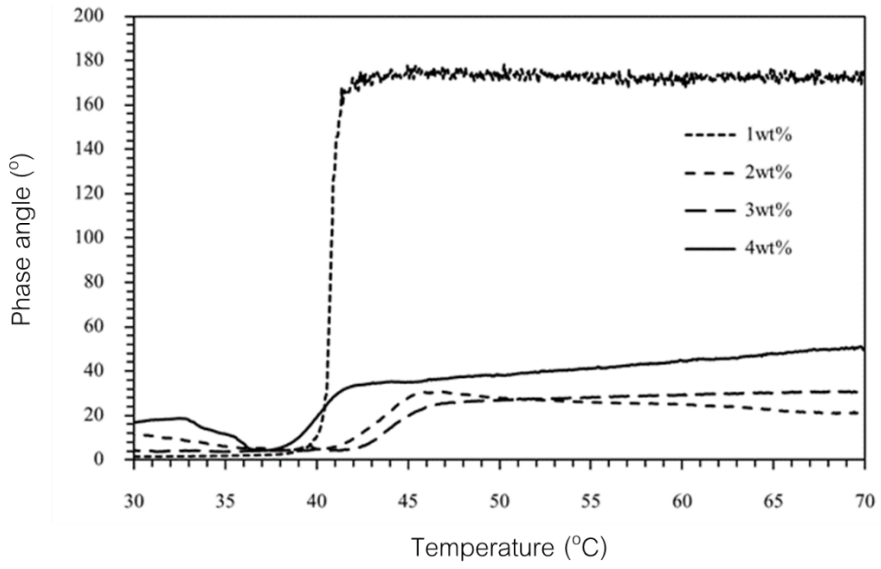


**Fig.4.2.3** Phase angle of ink prepared from different concentration of agar solution at 1, 2, 3 and 4wt%

**Fig.4.2.1** at 1wt% concentration of agar solution showed the temperature decreasing from 70 $^{o}$C cooling down to 40 $^{o}$C indicating that the storage modulus (G') lower than 1 Pa that was too low because of too much water in ink mixture being the unusual behavior. It was clearly observed in the preparation step, the $Al_2O_3$ particles was precipitated being the unsuitable behavior for printing.

For other ink mixtures, the storage modulus (G') was steady from 70 to 45 $^{o}$C. When the temperature was lower than 45 $^{o}$C, the storage modulus rose sharply. Therefore, the temperature of 50 $^{o}$C was selected in printing because storage modulus showed no change. The proper temperature was facilitated for extruding through nozzle and rapidly transforming to gel state. It was able to keep the shape of filament — good fidelity. In other words, fidelity or shape fidelity described the shape retention of single filaments upon extrusion compared to the original computer design and is sometimes referred to as print accuracy [47]. The storage modulus trend to divide into 2 groups of agar solution concentration.

1) At ≤ 3wt%

The degree of storage modulus between 70 to 45 $^{o}$C was less than 10 Pa for all the ink mixture. After the temperature reached 45 $^{o}$C and then decreased to 30 $^{o}$C, the storage modulus was sharply increased in range of 1000 and 10000 Pa

2) At ≥ 4wt%

The degree of storage modulus was about 100 Pa in range of 70 to 45 $^{o}$C. However, the storage modulus showed a slight increase only from 200 to 3000 Pa.

The tendencies of storage modulus were described from direct relationship between concentration of agar solution and storage modulus behavior. It was found that when the small amounts of agar molecules compared with $Al_2O_3$ particles in ink mixtures, the storage modulus behavior was under governed by the $Al_2O_3$ particles being the property of a solid or more precisely elastic property. While the ink mixture transformed to gel phase, the behavior of elastic solid was prominent. The storage modulus at 4wt% was affected by

the increasing amount of agar molecule in ink mixture. It was noticeable that the storage modulus did not sharply increase because the agar gel might be sufficient to determine the elastic property in the ink mixtures.

Considering at all concentration of agar solution concentration, although at 3wt% concentration clearly observed in **Fig.4.2.1** which was higher than at 4wt% concentration in range of 45 towards 30$^{o}$C. However, the decreasing temperature from 70 to 45 $^{o}$C rather provided low storage modulus of about only 10 Pa for 1, 2, and 3wt% but at 4wt% was high being about 100 Pa as shown in **Fig.4.2.2** and **Fig.4.2.3**.

When considering the relationship between the **Fig.4.2.1**, **Fig.4.2.2** and **Fig.4.2.3**, it was found that the unusual trend at 1wt% resulted from a lot of water containing in $Al_2O_3$ slurry ink. **Fig.4.2.1** showed that the storage modulus increased for the temperature decreasing of 45 to 30$^{o}$C, present the heat storage ability of solution transforms to gel state consistent with **Fig.4.2.2** of loss modulus that means heat loss or heat release. Therefore, the relation between storage modulus and loss modulus presented in terms of elastic and viscous behavior, respectively. The elastic and viscous behavior simultaneously exhibited were measured as shown in **Fig.4.2.3** indicating the phase angle represented by tanδ. Ink typically acted as viscoelastic properties when $0<\delta<90$ $^{o}$C [48].

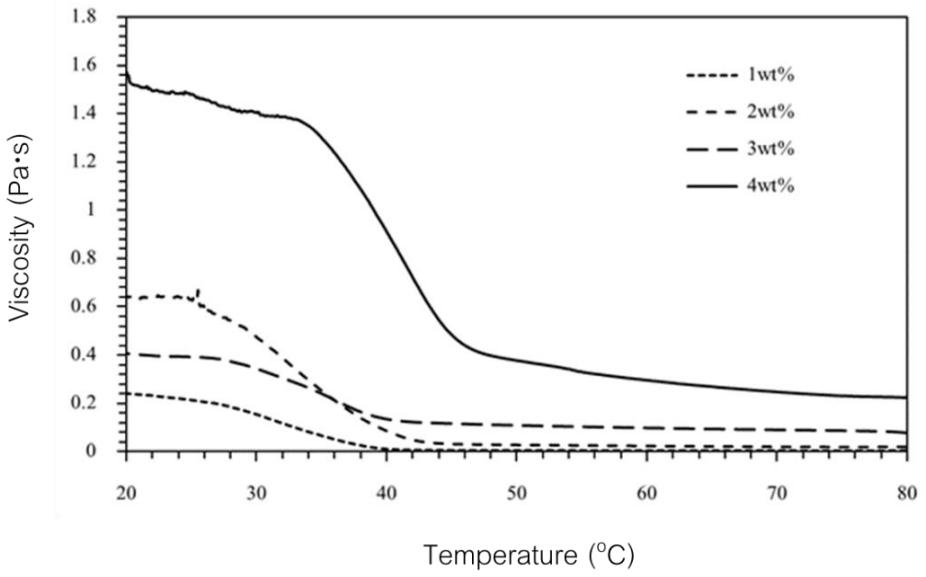


**Fig.4.2.4** Viscosity of ink prepared from different concentration of agar solution at 1, 2, 3 and 4wt%

The optimum concentration of agar solution was examined as shown in **Fig.4.2.4**. The viscosity of all the prepared solutions increased in range between 45 and 26°C, except for the solution with 4wt% concentration that increased from 46 to 34 °C. For viscosity, the behavior acts in the same way as the which divide into 2 groups. At ≤ 3wt% concentrations of agar solution, the temperature decreased from 70 to 45°C, the viscosity rather low no more than 0.2 Pa·s then the temperature gradually down to 45°C, the viscosity was gradually increase between 0.2 and 0.7 Pa·s. At ≥ 4wt% concentration of agar solution, when the temperature decreased from 70 to 45°C, the viscosity gradually increased between 0.2 and 0.5 Pa·s. After the temperature lowered during 45 and 30 °C, the viscosity clearly rose sharply to 1.4 Pa·s

Moreover, agar solution concentrations had effect on the viscosity. The higher concentrations of agar solution meant more chance of interaction between agar molecules.

In this study, rheological properties of ink were shown in terms of viscoelastic behavior. The proper viscosity was important to extrusion of ink in printing without problems such as bubbles in the plugger and pipe during extrusion due to the ink paste movement resulting in friction between the texture of ink paste with the surface of the inner tube wall and then creating clogging during extrusion. The proper viscosity was to avoid the collapsed printing [49]. As shown in **Fig.4.2.5**

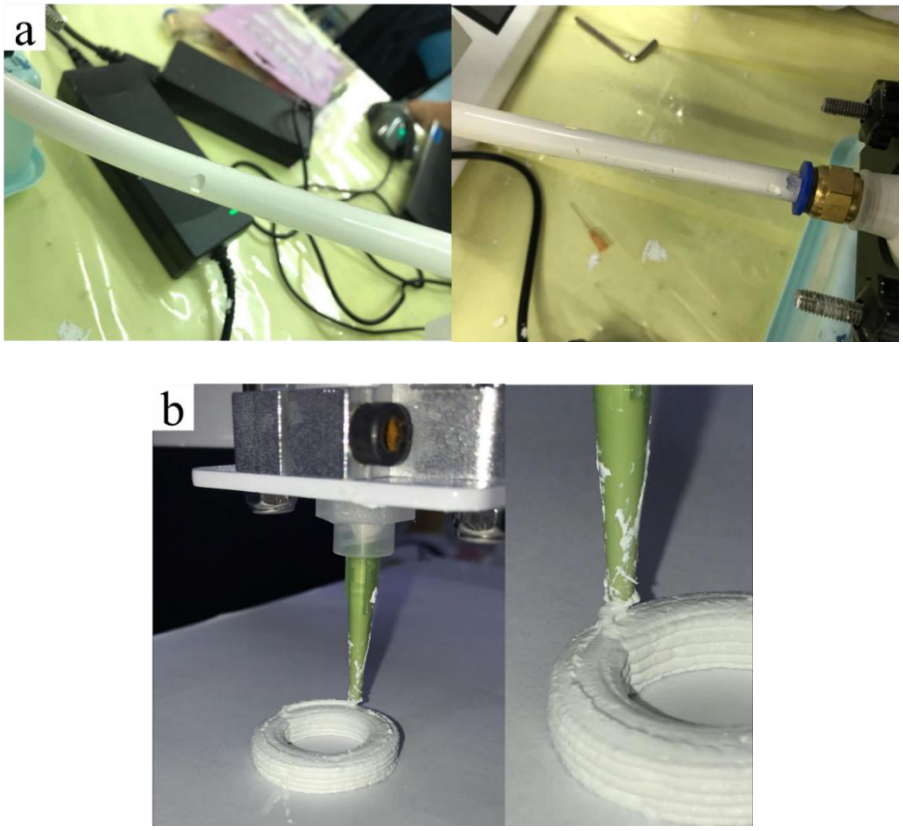


**Fig.4.2.5** Obstacles while working in printing a) bubbles and b) intermittent and clogging nozzle

The results of the experiment demonstrated that when the concentration of agar solution was at 4wt%, the viscoelastic of ink was optimal in comparison to the concentrations at ≤ 3wt%. On the contrary, a low concentration of agar solution showed no capability to shape or no gel formation, especially at 1wt% concentration acting like a liquid

and causing the settlement of $Al_2O_3$ particles rapidly. The poor results of printing was in line with the storage modulus degree lower than 1 Pa in the range of 70 and 40$^oC$. The storage modulus at lower than 40$^oC$ was increased to approximately to 1000 Pa seing the unsuitable behavior for printing because of too much water in the ink mixture at 1wt% concentration of agar solution. Therefore, the concentration of agar solution at 4wt% was selected for printing at 50$^oC$ preventing the agar solution transformation to gel before printing.

### 4.3 Ink paste

The rheology results were discussed and used for improving the ink paste with additives addition and liquid reduction in the ink. The ink paste preparation followed the preparation of subsection 3.2.1 part I and II. After obtaining the clear yellow agar solution, the additives were added, i.e. addition of acetone, HEC, and PEG1500, respectively.

Previously, the preliminary experiments without the HEC addition into agar solution found that the gel-forming samples occurred due to the agar properties. This result made it unable to print because the solidification of sample from gelation was clogged at the nozzle tip. For printing, the printing temperature of ink paste must not form the gel state prior to injecting out of the nozzle. In this case, the addition of HEC eliminated the need to maintain the temperature of the ink paste, including helped increase the optimal viscosity of ink paste for printing obviously. The viscosity of ink paste was improved by addition of HEC due to its characteristic of thickening. The suggestion usage was 0.5-3% which soluble in water but insoluble in organic solvents [50][51]. Therefore, this result of HEC addition varied at 0, 1, and 2wt% of solid loading of agar powder was studied together with the addition of 10wt%PEG1500 of solid loading of agar powder. It was found that 2wt%HEC addition presented the optimal viscosity behavior. The $Al_2O_3$ ink paste containing 2wt%HEC showed clearly the increase in viscosity after adding HEC, that is suitable 3D printing. However, the higher viscosity obtained from the 2wt%HEC addition influenced in the HEC mixing step. **Fig.4.3.2** and **Fig.4.3.3** exhibited the small clusters dispersed in

agar solution which able to clearly observe after HEC adding. At 2wt%HEC adding, the existence of clusters were more than 1wt%HEC. It might be the solubility limit in solution due to 4wt%agar solution is highest concentration of agar. Therefore, adding more HEC into agar solution resulting in an agglomeration or the clusters of HEC molecules [46]. Whereas, the ink paste without the HEC addition showed no the cluster or agglomeration.

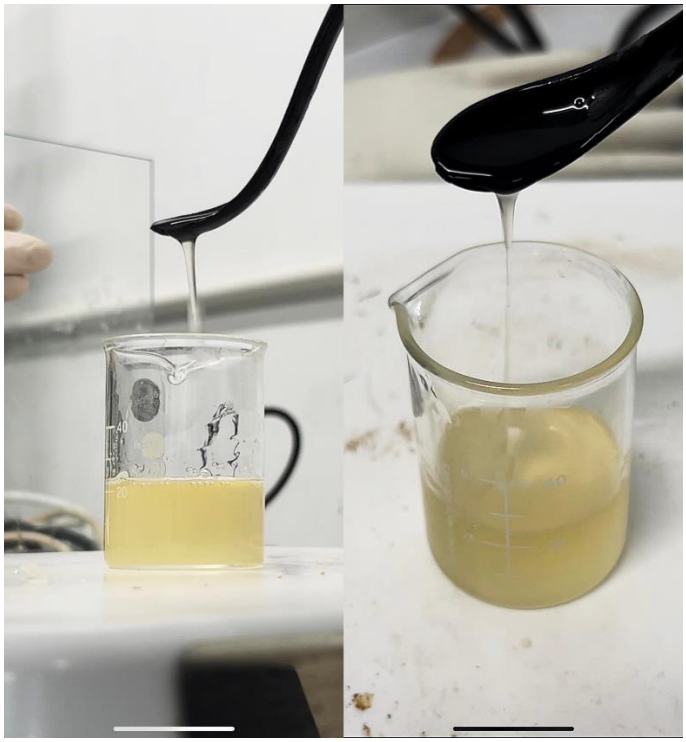

**Fig.4.3.1** The mixed agar solution containing 10wt%PEG1500

**Fig.4.3.2** The mixed agar solution containing 1wt%HEC and 10wt%PEG1500

**Fig.4.3.3** The mixed agar solution containing 2wt%HEC and 10wt%PEG1500

To enhance the fidelity of printed sample, acetone was added as a drying agent. Acetone was soluble in water because of the carbonyl group in structure of acetone molecules able to bonded on water molecules by hydrogen bonds. The results from carbonyl ability in acetone structure allowed to accept the hydrogen bond from molecules of other compound including water molecules. Additionally, O-H group of water is favorable in acetone and water interaction into solution form [52].

The acetone addition varied at 0, 10, and 20wt% which acetone volume was calculated from the basis of the total agar solution weight and convert to volume in addition. After acetone was completely soluble in the clear agar solution, 2wt%HEC and 10wt%PEG1500 was added. Each additives needed to be added in sequence and must stirring by magnetic bar to be completely dissolve before adding another additive. The reason for the first addition of acetone was that it was dissolvable in agar solution as mentioned before [53][54][55][56].

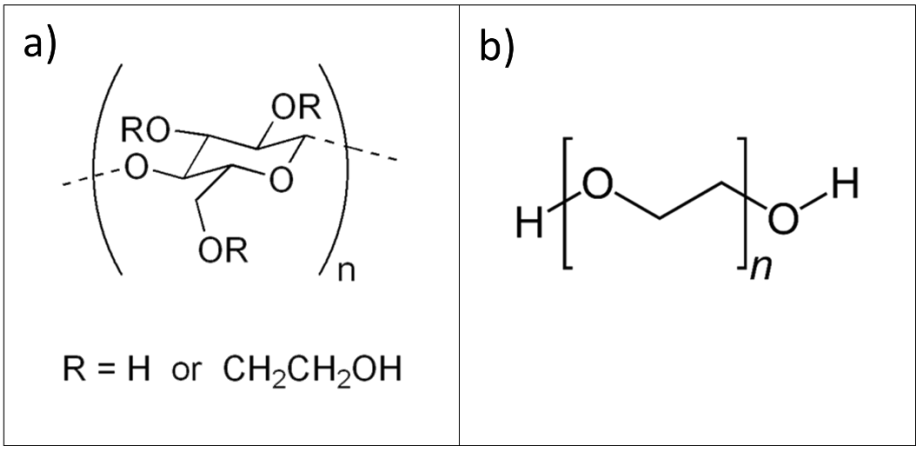


**Fig.4.3.4** Chemical structure of a) hydroxyethyl cellulose (HEC), and b) polyethylene glycol1500 [57] [58]

Moreover, the addition of PEG1500 helped in act as a lubricant inside the PVC tube**.** Both HEC and PEG1500 were non-ionic polymer and soluble in water but HEC and PEG1500 were insoluble and soluble in organic solvents, respectively. The PEG1500

was hydrophilic polymer able to dissolve in solution which contains water [59][60][61][62]. Additionally, the prepared solution possessed the high viscosity after adding HEC before adding PEG1500. However, after PEG1500 was added, the viscosity of solution slightly decreased again. Therefore, the physical behavior of ink pastes with and without acetone was not different after adding of PEG1500.

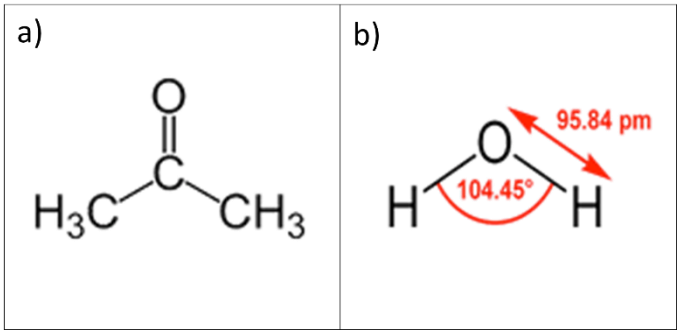


**Fig.4.3.5** Chemical structure of a) acetone molecule, and b) water molecule

Acetone at 10wt% of the total agar solution weight is optimal in preparing the ink paste which selected from varying at 0, 10, 20wt%. After the $Al_2O_3$ ink paste printing, green body samples keep drying in air for 24 h. The samples were dried in oven at 110$^{o}$C to ensure completely drying and reducing the problem of cracking in samples due to the rapid evaporation of water in the green body samples resulting in the shrinkages. The sintering step was performed at 1300$^{o}$C to burn the binder out off the green body samples and increase the strength of samples. The grain growth with heating rate 5 $^{o}$C/min begins at room temperature elevated to 1300$^{o}$C and holding time at 1300$^{o}$C for 1 h. to sinter and necking of the particles.

For the ink paste improving by 0, 1, and 2wt%HEC and 10wt%PEG1500 without acetone addition indicate that the sample cracked only as **Fig.4.3.8** because at 2wt%HEC means that too much of HEC content. Large amount of polymer chain of HEC is ability to form gel texture and increase viscosity from water storage which excellent water retention. It might be approach to crack in sample after water rejection. Considering without acetone condition, 0 and 1wt%HEC means no HEC exists at all and small amount of HEC, respectively. Only 0wt%Acetone and 1wt%HEC with 10wt%PEG1500 added in agar

solution which will not cracking because able to soluble in agar solution without exceeding the solubility limit.

All substance in agar solution mixture, both HEC and PEG1500 are polymer including agar powder themselves also a polymer. When their polymer was added more in agar solution by varying of 0, 1, and 2wt% HEC, at the highest solubility limitation is 2wt% HEC present the optimal viscosity behavior but effect on physical of solution which agreeable with the agglomerate occurring due to over the limit of solubility of polymers in water from large amount of polymer in solution.

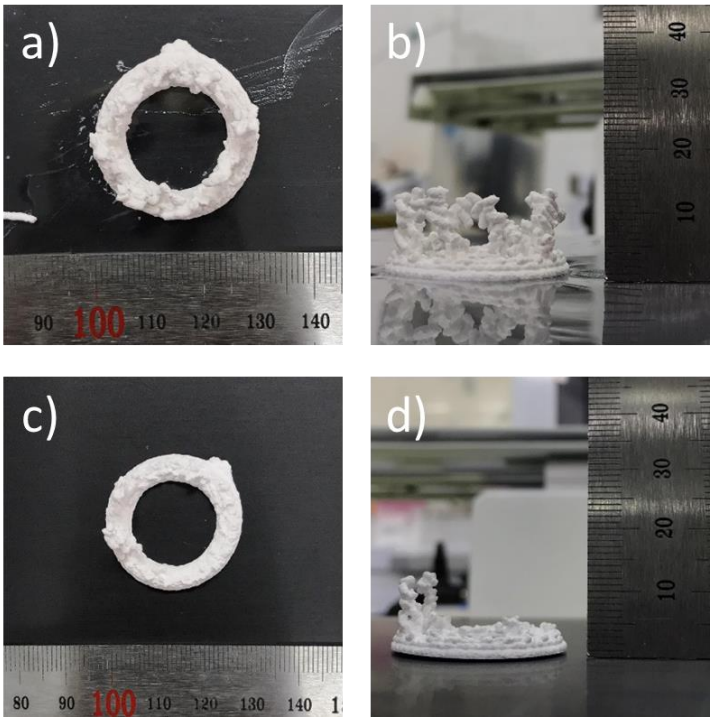


**Fig.4.3.6** Printed samples after improving ink paste with 10wt%PEG1500; a) after printing (top view), b) after printing (side view), c) after sintering (top view), and d) after sintering (side view)

The appearance of printing ink filament as shows in **Fig.4.3.6.** Due to ink paste with no adding of HEC, viscosity behavior given by agar properties of gel structure. The Ink paste without HEC still present the behavior of high viscosity until gelation. After removing of ink paste mixture from under mixing at 60$^{o}$C, temperature was rather decrease

to room temperature leading to gel forming. In other words, ink paste mixture unstable at room temperature. While the ink paste operates on 3D printer, the temperature already reduces to gel forming temperature. High pressure was required to press ink paste out for performing printing because the increasing viscosity. High viscosity of ink difficult to press through the small tip of nozzle only 1.5 mm diameter size. The ink pastes filament incomplete in printing that tear and discontinuous filament as show in **Fig.4.3.6** of after printing able to observe. For after sintering, sample strength was increased.

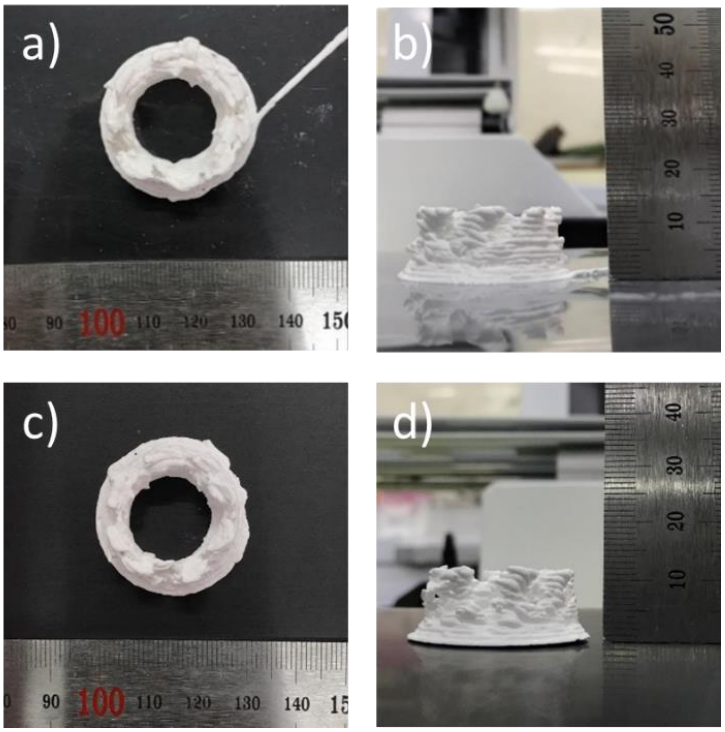


**Fig.4.3.7** Printed samples after improving ink paste with 1wt%HEC and 10wt%PEG1500; a) after printing (top view), b) after printing (side view), c) after sintering (top view), and d) after sintering (side view)

Because of **Fig. 4.3.7** (a, b, c, and d), the ink paste had a high viscosity than **Fig. 4.3.6**. Printed samples have an uneven texture from the ink paste filament. Even without acetone and 10wt%PEG1500, the addition of 1wt%HEC partially soluble and

acceptable content in soluble including to help for increase viscosity due to swelling from water absorption.

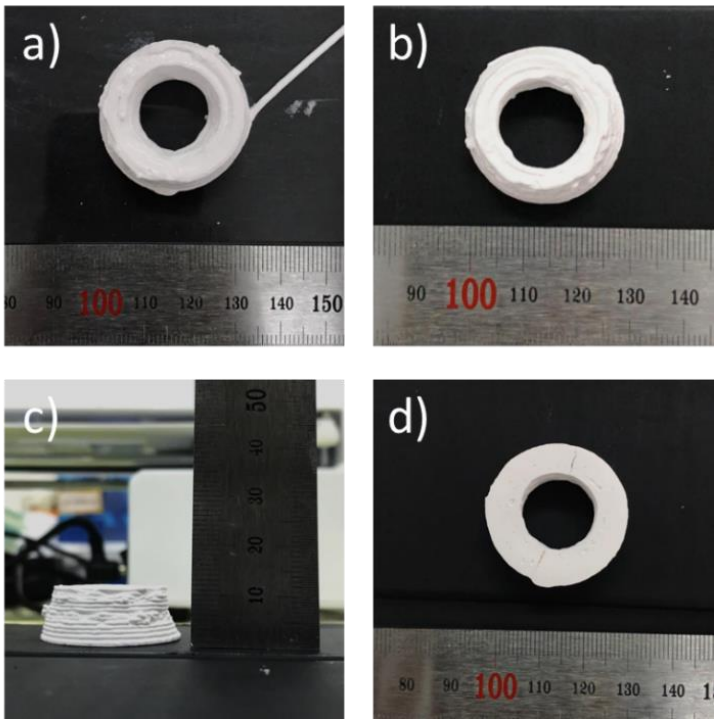


**Fig.4.3.8** Printed samples after improving ink paste with 2wt%HEC and 10wt%PEG1500; a) after printing (top view), b) after sintering (top view), c) after sintering (side view), and d) after sintering (bottom view)

2wt%HEC content presents a suitable viscosity which optimum for shaping and layering up ink paste printing, as was evident from the ink paste filament after samples were printed. **Fig.4.3.8 c)** shows the ink paste filament printing, which has a better shape than **Fig.4.3.6** and **Fig.4.3.7**. Even though very high viscosity had a good ability to form but was not good for drying, resulting in cracks on the bottom of the sample; might be possible that over of HEC content unable to dissolve in solution and lead the way to break of sample.

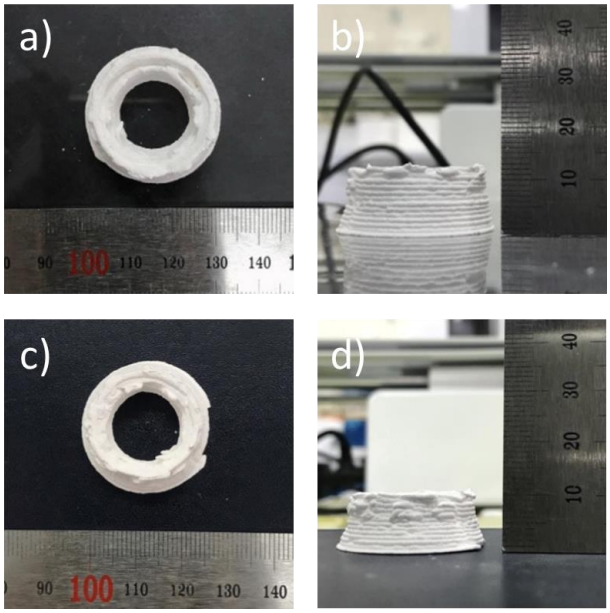


**Fig.4.3.9** Printed samples after improving ink paste with 10wt%acetone 2wt%HEC 10wt%PEG1500 a) after printing (top view), b) after printing (side view), c) after sintering (top view), and d) after sintering (side view)

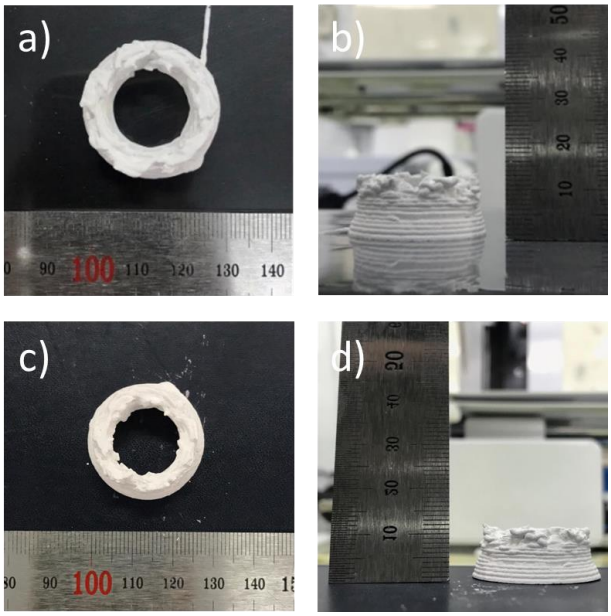


**Fig.4.3.10** Printed samples after improving ink paste with 20wt%acetone 2wt%HEC 10wt%PEG1500 a) after printing (top view), b) after printing (side view), c) after sintering (top view), and d) after sintering (side view)

Considering the selecting of optimum viscosity in condition of 0wt%acetone 2wt%HEC 10wt%PEG1500 in **Fig.4.3.8.** At 2wt%HEC content was suitable viscosity behavior and they were added combined acetone at 10 and 20wt% to assist in drying rapidly. **Fig.4.3.9 and Fig.4.3.10** were found that a good shape printing but when adding of acetone does not observe in printing. **Fig.4.3.8** have cracking problem since too much of HEC content but after adding of acetone which help to solves cracking problem that **Fig.4.3.9 and Fig.4.3.10** similarly printed shape in obviously and show a better texture of shaping.

## 4.4 Microstructure

The microstructure of the printed samples was observed by Scanning Electron Microscope or SEM (JSM 5800LV, JEOL, Netherlands) at 20 kV. The preparation of sintered samples for SEM were cut with SiC cutting wheel and the cut samples were dried in an oven at 110$^{o}$C for 24 h. Then the samples were coating of gold on surface using 2-time sputtering for 60s each.

The SEM image microstructure confirm and support the reason of printed samples in part 4.3. as follows;

Comparison microstructure of 10wt%PEG1500 without acetone adding varying at 0, 1, and 2wt%HEC, respectively at same magnification of 2000X.

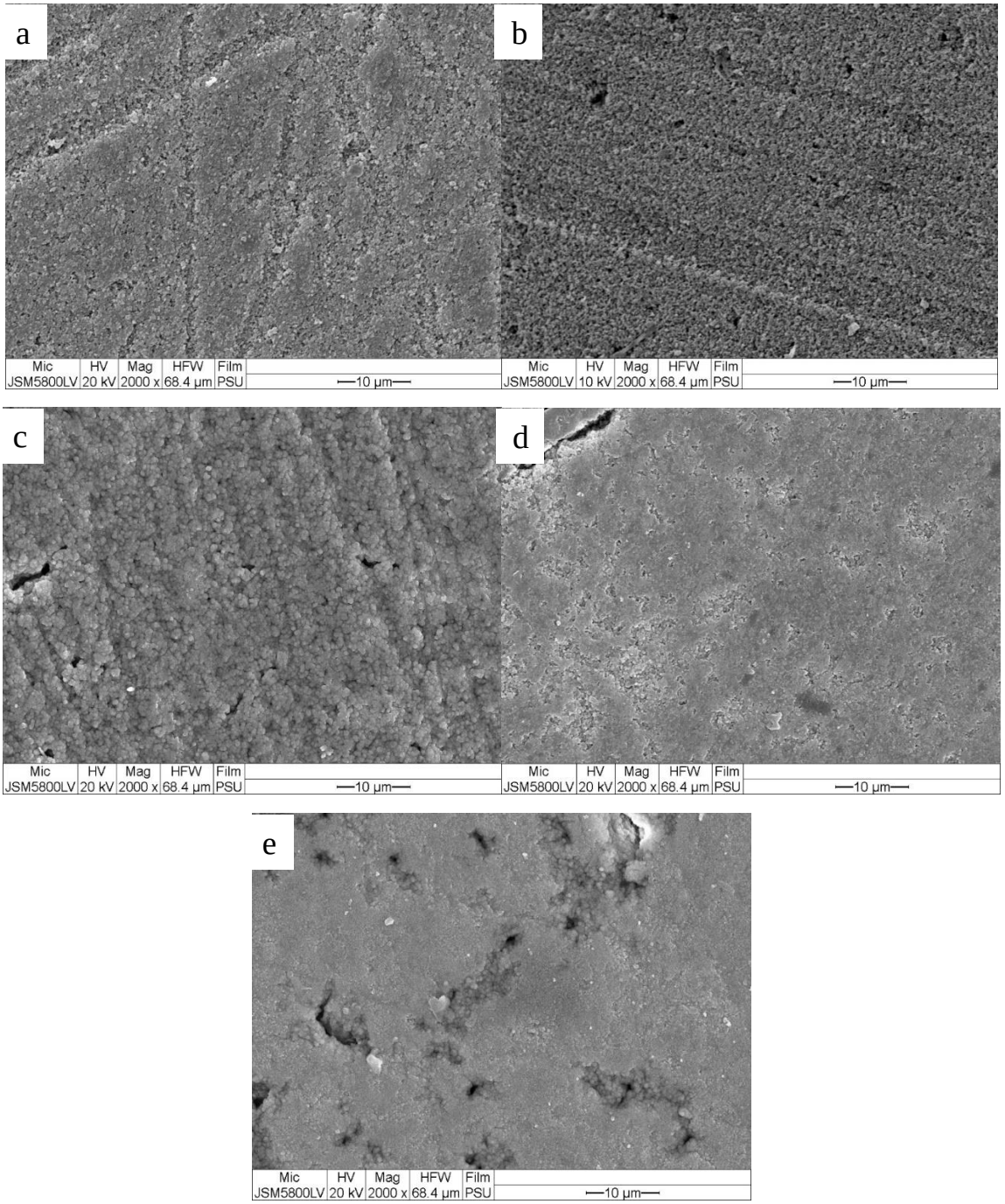


**Fig.4.4.1.** Microstructure at 2000X of a) 10wt%PEG1500, b) 1%HEC and 10wt%PEG1500, c) 2%HEC and 10wt%PEG1500, d) 10%acetone, 2%HEC and 10wt%PEG1500, and e) 20%acetone, 2%HEC and 10wt%PEG1500

The SEM image with 2000X of magnification show the different of %HEC content. Indicate that the particles were uniformly and tightly disperse. Moreover, the observation was clearly show dense different of particles dispersion. **Fig.4.4.1 a)** at 0wt%HEC of sintered sample show the dense sintered particles probably the viscousness of gel formed when temperature decrease to gelling temperature, the $Al_2O_3$ particles in ink paste mixture forming shape by agar structure. Before printing, the ink paste mixture present a high viscosity because alumina particles to be tight together from agar gel structure. The ink paste forming shape was pressed through the nozzle is quite difficult.

Confirming the different between **Fig.4.4.1 d) and e)** by SEM image microstructure. The ink paste improving by 2wt%HEC was selected which obtained highest viscosity behavior. At 2wt% HEC was further improved by adding acetone for rapid drying. Comparison at 2wt%HEC with varying of 0, 10, and 20wt%acetone. **Fig.4.4.1 d) and e)** for the observation in part 4.3, printed shape does not different but the different show on SEM image indicate that particles densely distributed at higher wt% of acetone content.

## 4.5 Physical properties of printed samples

The ink paste improving by additive adding exhibited the physical behavior of shrinkage which effects on density. The printed samples before and after sintering were different of size due to shrinkage when samples completely dried.

Considering the composition of HEC varying at 0, 1, and 2wt% with 0wt%acetone and 10wt%PEG1500. **Fig.4.5.1,** the apparent density trend to decrease but bulk density trend to increase according to the increase amount of HEC. The apparent and bulk density were related with adding of HEC content because at higher HEC indicate that the more amount of polymer was added which chemical structure of HEC has a hydroxyl group in polymer chain for reacts with other HEC molecules. At 2wt%HEC without acetone addition was lowest apparent density by obviously corresponding with SEM image microstructure. Too much of HEC molecule might be not dissolve at all. According to the discussion in part.4.3, the reason of too much HEC were not dissolves because exceeded the solubility limit which lead to combine molecule of HEC themself. The agglomeration

or cluster of HEC molecules were repulsed each other from negative charge of hydroxyl group and able to instead between gap of other molecules. Thus, the reason of the distance between each molecule was affected apparent density to decrease which agreeable the %firing shrinkage (%FS) as **Fig.4.5.2.** was increased with increasing of HEC that means higher HEC in composition of ink paste mixture more bubbles or vacancy approach to shrink a lot after samples was dried. The printed samples after sintered will present the tendency value of apparent density decreased and bulk density increased. Due to the apparent density measured bulk and closed pore but bulk density measured all of closed and opened pore, bulk including the defects. However, without HEC adding were not affect same the reason as mention or comparable with low of HEC content. Therefore, the ink paste composition at 2wt%HEC was considered because highest value of bulk density corresponding to the reason of rheological behavior.

The improving of ink paste composition by varying of acetone at 0, 10, and 20wt% with 2wt%HEC and 10wt%PEG1500 were also considered both of apparent and bulk density. **Fig.4.5.1,** indicated that higher amount of acetone addition effect to increase apparent density related to decrease %firing shrinkage (%FS). Describing under the condition of acetone varying at 0, 10, and 20wt% that when increasing of acetone effect small amount of porosity which less shrinkage as **Fig.4.5.2.** The reason means lead to more densely of apparent density but bulk density was decreased because the samples were calculated include open pore and also other defects. Moreover, at 0wt%acetone or without acetone adding means the vacancy between helices structure between long polymer chains in agar role as store water which still exceeds the solubility of HEC. Therefore, the influent of acetone adding not only solves problem of cracking in printed sample but also rapidly drying.

**Fig.4.5.2** show %Apparent porosity ($\%P_A$) and %water absorption ($A_w$) were reduced when increasing of HEC content. $\%P_A$ is an apparent porosity consisted of all porosity in samples which can be replaced by water. Indicated that higher HEC content effect on $\%P_A$ to decrease. Due to high HEC also means high of polymer in composition indicate that before drying the porosity was formed in samples from water storage of

polymer as water swelling. After drying, samples shrink leading to decrease their bubbles from water evaporation. Therefore, higher HEC content given lower apparent porosity. There reason also approach more shrinkage which corresponding to water absorption ability. %Water absorption ($A_w$) were reduced at higher HEC content because high HEC able to store water a lot, the shrinkage a lot also. The dried samples were decreased porosity volume for water absorption which water can be replaced in.

For acetone varying**, Fig.4.5.2** explained the %Apparent porosity (%$P_A$) and %Water absorption ($A_w$) trend to increase as when acetone content increasing. At optimal of ink paste improving at 2wt%HEC, apparent porosity was increased when increasing of acetone. Because of acetone added in mixtures, acetone also role as a liquid one in mixtures or liquid content in mixture was increased. According to removes liquid out both acetone and water by evaporation, after completely dried means the missing of liquid volume including other binder such as HEC and PEG1500 were created large amount of pore. The reason reaches more increasing of %apparent porosity appear as increase of acetone. The increasing amount of %apparent porosity were related to %water absorption ($A_w$) that when the dried samples was more porosity also means more space or vacancy for water replacing or water absorption. Therefore, at higher acetone content was exhibited increasing of %water absorption.

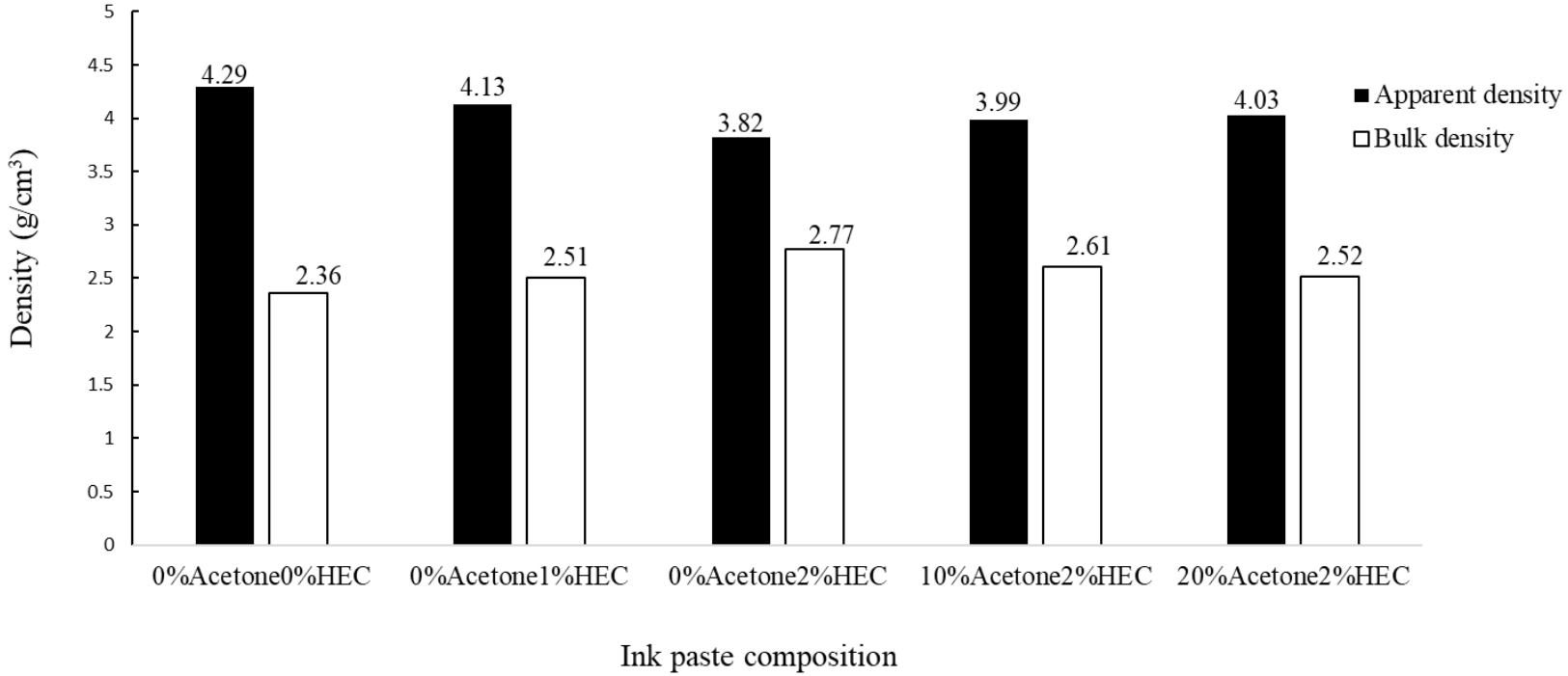


**Fig.4.5.1** Charts of apparent density, and Bulk density at different compositions

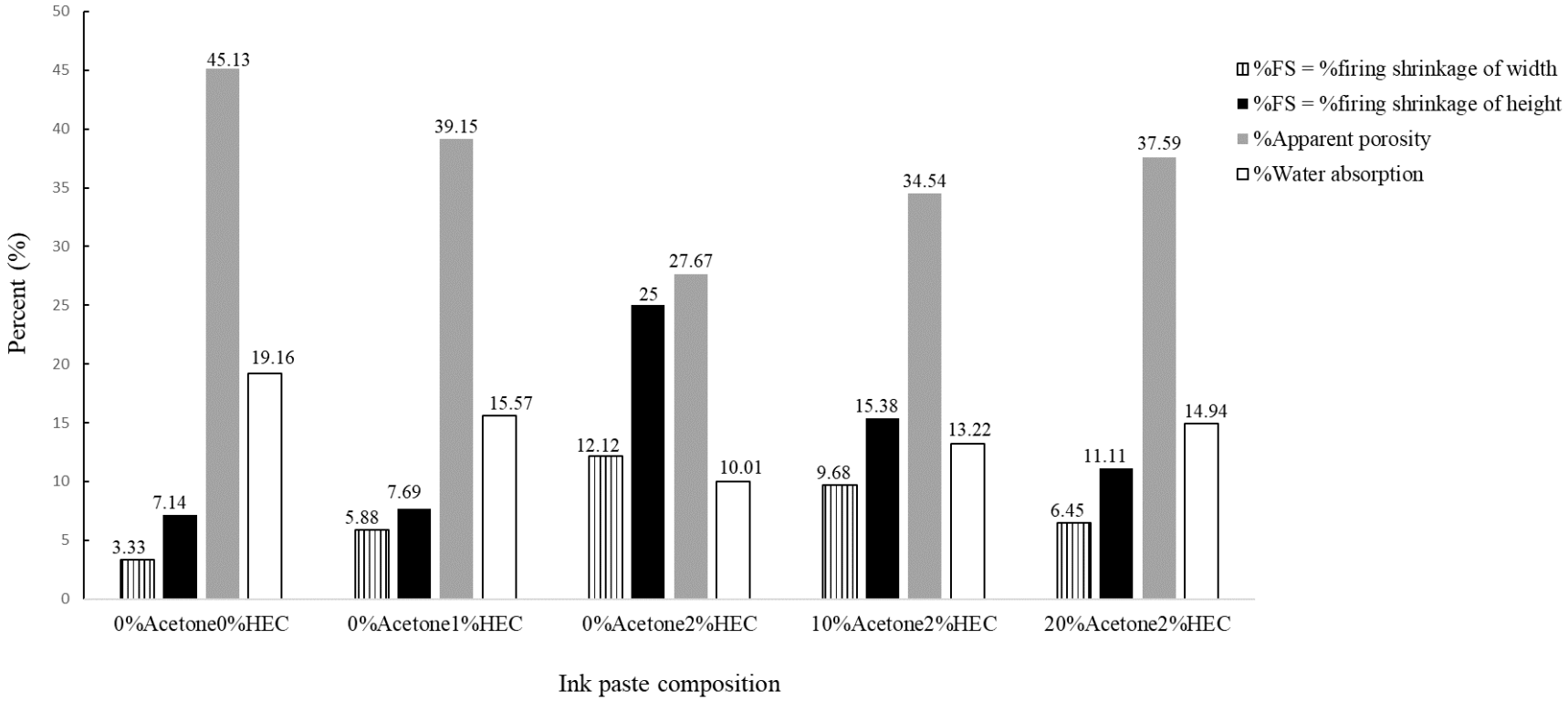


**Fig.4.5.2** Charts of %firing shrinkage, %apparent porosity, and %water absorption at different compositions

# CHAPTER 5

## 5. CONCLUSIONS

In this research, tubular $Al_2O_3$ membrane was fabricated by 3D printing as the so-called direct ink writing technique. This study was conducted in terms of the composition, additive content, rheological behavior, and characterization such as microstructure analysis, density, and shrinkage of sintered samples. The $Al_2O_3$ ink paste with 1wt% concentration of agar solution was unsuitable for further adjustment because of too much water in the printed mixture. The curve of G' and G'' tend to increase as the concentration of agar solution increase at 2, 3 and 4wt%, respectively. Whereas the degree of viscosity was highest at 4wt% concentration of agar solution corresponding with G' and G" value that are suitable for usage as ink paste printing.

Ink paste modified by HEC adding at 0, 1, and 2wt% with 10wt% PEG1500 which immediately observed the large amount of agglomeration at higher HEC content. The addition of 2wt% HEC was over solubility limit resulting in the occurrence of HEC clusters. HEC only help to improve viscosity which was appropriated for using as thickener in ink paste. The optimum HEC content at 2wt% was adjusted with agar solution at 4wt% with fixing 10wt%PEG1500 and varying 0, 10, and 20wt%acetone content. It could be seen that the increasing of acetone offered denser structure as supported by the SEM images.

The main benefit to be expected from the addition of acetone is the rapid drying of printed samples. However, the adding acetone also had effect on density after drying and sintering relevant to shrinkage, porosity, volume, and water absorption. The increase in acetone amount led to the reduced shrinkage. Therefore, the water absorption was increased when acetone added more and more due to the increased apparent porosity from the addition of acetone.

# REFFERENCES

[1] What Are the Different Types of 3D Printing. (n.d.). Future Learn. https://www.future learn.com/info/courses/getting-started-with-digital-manufacturing/0/steps/184102 (accessed 24 February 2023)

[2] What are the advantages and disadvantage of 3D printing. (n.d.). TWI-global. https://www.twi-global.com/technical-knowledge/faqs/what-is-3d-printing/pros-and-cons (accessed 24 February 2023)

[3] What is 3D printing? – Technology definition types. (n.d.). TWI-global. https://www.twi-global.com/technical-knowledge/faqs/what-is-3dprinting (accessed 24 February 2023)

[4] M.A. Green. 1987. High Efficiency Silicon Solar Cells. *Seventh E.C. Photovoltaic Solar Energy Conference* 1987: 681–687.

[5] Gupta, D. (Ed.). 2005. *Diffusion Processes in Advanced Technological Materials*. NORWICH, NEW YORK, U.S.A: Springer.

[6] Jean M., and Stephen W. H. 2002. *Theoretical Methods in Condencsed Phase Chemistry*: Springer Dordrecht.

[7] Wasim M. 2020. Advantages of Ceramic Membranes Filtration technology over Conventional Clarification andTe. Linkedin. https://www.linkedin.com/pulse/ advantages-ceramic-membranes-filtration-technology-over-mohammed (accessed 24 February 2023)

[8] Dj.M. Maric, P.F. Meier and S.K. Estreicher. Mater Sci. *Forum* 1992 (83-87): 119.

[9] R.J. Ong, J.T. Dawley and P.G. Clem. 2011. Chemical solution deposition of biaxially oriented (Ba,Sr)$TiO_3$ thin films on 〈100〉 Ni. *Journal of Materials Research* 2023 (10): 2310 – 2317

[10] What Are the Different Types of 3D Printing?. (n.d.). futurelearn. https://www.future learn.com/info/courses/getting-started-with-digital-manufacturing/0/steps/184102 (accessed 24 February 2023)

[11] Additive manufacturing (AM). (n.d.). weldlabs. http://www.weld.labs.gov.cn (accessed 24 February 2023)

[12] What is the 3D printing? – technology definition and types. (n.d.). twi-global. https://www.twi-global.com/technical-knowledge/faqs/what-is-3d-printing#Printing Processes (accessed 24 February 2023)

[13] Wikipedia. 2023. 3D printing. https://en.wikipedia.org/wiki/3D_printing (accessed 24 February 2023)

[14] Spiceworks. 2022. What Is 3D Printing? Working, Software, and Applications. https://www.spiceworks.com/tech/devops/articles/what-is-3d-printing/ (accessed 24 February 2023)

[15] What is 3D Printing?. (n.d.) 3dprinting. https://3dprinting.com/what-is-3d-printing/ (accessed 24 February 2023)

[16] All3dp. 2023. The 7 Main Types of 3D Printing Technology. https://all3dp.com/1/types-of-3d-printers-3d-printing-technology/#section-material-extrusion (accessed 24 February 2023)

[17] What are the advantages and disadvantage of 3D printing. (n.d.). TWI-global. https://www.twi-global.com/technical-knowledge/faqs/what-is-3d-printing/pros-and-cons (accessed 24 February 2023)

[18] Advantages of 3D printing (and disadvantages). (n.d.). tractus3d. https://tractus3d.com/knowledge/learn-3d-printing/advantages-of-3d-printing/ (accessed 24 February 2023)

[19] Advantages and Disadvantages of 3D Printing. (n.d.). javatpoint. https://www.javatpoint.com/advantages-and-disadvantages-of-3d-printing (accessed 24 February 2023)

[20] Which 3D printing technologies do you use?. (n.d.). statista. https://www.statista.com/statistics/560304/worldwide-survey-3d-printing-top-technologies/ (accessed 24 February 2023)

[21] Makeuseof. 2022. FDM vs. SLA: The Differences Between Filament and Resin 3D Printers. https://www.makeuseof.com/fdm-vs-sla-the-differences-between-filament -and-resin-3d-printers/ (accessed 24 February 2023)

[22] What Are the Different Types of 3D Printing?. (n.d.). futurelearn. https:// www. futurelearn.com/info/courses/getting-started-with-digital-manufacturing/0/steps/184102 (accessed 24 February 2023)

[23] Matt A. 2019. Types of 3D Printing Technology. Protolabs. https:// www.protolabs.com/resources/blog/types-of-3d-printing/ (accessed 24 February 2023)

[24] What is FDM (fused deposition modeling) 3D printing?. (n.d.). hubs. https:// www.hubs.com/knowledge-base/what-is-fdm-3d-printing/ (accessed 24 February 2023)

[25] 3D Printing and Additive Manufacturing Services Information. (n.d.). globalspec. https://www.globalspec.com/learnmore/manufacturing_fabrication_services/part_fabrication_services/additive_manufacturing_services (accessed 24 February 2023)

[26] Hehan X, Xianfeng Y, Peng L, Xiewen X, Zhe Z, Wei Z, and Zhijian S. 2021. 3D gel printing of alumina ceramics followed by efficient multi-step liquid desiccant drying. *European Ceramic Society* 41 (13): 6634-6640.

[27] Julkarnyne M. Habibur R, MD Nahin Islam S, Kumkum A, Ajit K, Masaru K, and Hidemitsu F. 2020. Rheological and mechanical properties of edible gel materials for 3D food printing technology. *Heliyon* 6 (12): 05859.

[28] A. Paterlini, S. Le Grill, F. Brouillet, C. Combes, D. Grossin, G. Bertrand. 2021. Robocasting of self-setting bioceramics: from paste formulation to 3D part characteristics. *Open Ceramics* (5): 100070.

[29] Jilong W, Yan L, Xintian Z, Syed Ehsanur R, and Siheng S. 2021. 3D printed agar/ calcium alginate hydrogels with high shape fidelity and tailorable mechanical properties. *Polymer* (214): 123238.

[30] Christophe G, Tarek S, Søren Bredmose S, Vincenzo E, Jacob R. B, and Astri Bjørnetun H. 2021. Hybrid inks for 3D printing of tall $BaTiO_3$-based ceramics. *Open Ceramics* (6): 100110.

[31] Dipjyoti S, and Suvendu B. 2010. Hydrocolloids as thickening and gelling agents in food. *Association of Food Scientists & Technologists* 47(6):587–597.

[32] Jelena J. Gulicovski, Ljiljana S. erovi, and Slobodan K. Milonji. 2008. Point of Zero Charge and Isoelectric Point of Alumina. *Materials and Manufacturing Processes* 23 (6): 615-619.

[33] Glauco M. L, Guilhermina Ferreira T, J.P.C. Costa, and L. Perazolli. 2017. *Electrophoretic Deposition (EPD).* New York: Nova science publishers.

[34] He L. and Carl P. Tripp. 2008. Detection of Bacillus globigii Spores Using a Fourier Transform Infrared–Attenuated Total Reflection Method. *Applied Spectroscopy* 62 (9): 963-967.

[35] Lavanya A, Yee-Kwong L, and Andy F. 2014. Kaolin particles with $Ca2^+$ – Contributory effects of Alumina and Silica Sheets. *Chemeca.*

[36] Justyna Z, Marcin W, Aleksandra M, and Paulina P. 2020. Microstructure and mechanical properties of $Al_2O_3$-Cu-Ni hybrid composites fabricated by slip casting. *Processing and Application of Ceramics* 14 (1): 1–8.

[37] George V. F, and Yang G. 2007. Charging Behavior at the Alumina–Water Interface and Implications for Ceramic Processing. *American Ceramic Society* 90 (11): 3373–3388.

[38] Rafael Kenji N, Ellen R, Mara Gabriela Novy Q, Dachamir H, Kurosch R, and Michaela W. 2021. Effect of MgO on the microstructure and properties of mullite membranes made by phase inversion tape casting. *Asian Ceramic Societies* 9 (3): 1228-1238.

[39] Yingchao D, Stuart H, Jian-er Z, Zhanlin J, Jiandong W, and Guangyao M. 2011. Sintering and characterization of flyash-based mullite with MgO addition. *European Ceramic Society* (31): 687–695.

[40] Yash Hemant P, Manish B, and Anushka S. 2022. Agar-agar extraction, structural properties and applications. *The Pharma Innovation* 11 (6): 1151-1157.

[41] Nobuyuki I, and Hodaka U. 2020. Concentration dependence of the sol-gel phase behavior of agarose-water system observed by the optical bubble pressure tensiometry. *Science report* 10 (1): 2620.

[42] Hydrocolloid. (n.d.). foodnetworksolution. https://www.foodnetworksolution.com/wiki/word/0375/hydrocolloid%E0%B9%84%E0%B8%AE%E0%B9%82%E0%B8%94%E0%B8%A3%E0%B8%84%E0%B8%AD%E0%B8%A5%E0%B8%A5%E0%B8%AD%E0%B8%A2%E0%B8%94%E0%B9%8C (accessed 16 September 2022)

[43] Gelling agent. (n.d.). Prince of Songkla University Pattani Campus. https://kb.psu.ac.th/psukb/bitstream/2010/9183/6/Chapter2.pdf (accessed 16 September 2022)

[44] En wikipedia. 2023. Agar. https://en.wikipedia.org/wiki/Agar (accessed 16 September 2022)

[45] Chemical and Physical Properties of Agar in Cooking. (n.d.). scienceofcooking. https://www.scienceofcooking.com/chemical_physical_properties_agar.htm (accessed 16 September 2022)

[46] Cameron D. M, and Kevin P. P. 2011. Agar-Based Aqueous Gel Casting of Barium TitanateCeramics. *Applied Ceramic Technology* 8 (3): 597-609.

[47] Andrea S, Riccardo L, Matteo D'Este, Susanna P, David E, and Jos M. 2020. Printability and Shape Fidelity of Bioinks in 3D Bioprinting. *Chemical Reviews.*

[48] Nisapha K. 2546. *Polymer science*. National Metal and Materials Technology Center.

[49] Zhenyu Y, Chengyi C, Diwei Z, Siwei M, Jianjun G, Yuchuan C, Gaojie X, Zhixiang L, and Aihua S. 2021. Study on 3D-Direct Ink Writing based on adding silica submicron-particles to improve the rheological properties of alumina ceramic ink. *Materials Today Communications* (28): 102534.

[50] Hydroxyethylcellulose (HEC). (n.d.). windypointsoap. https://www.windy pointsoap.com/ products/hydroxyethylcellulose-hec (accessed 25 January 2023)

[51] Hydroxyethyl Cellulose (HEC, HMHEC) Properties and applications. (n.d.). polymerdatabase . https://polymerdatabase.com/Polymer%20Brands/HEC.html (accessed 25 January 2023)

[52] Solubility Theory. (n.d.). utsc.utoronto. https://www.utsc.utoronto.ca/webapps/ chemistryonline/production/solubility.php?fbclid=IwAR3rvQuh73NZYp49a8jTgb_QGqjO xiyi1C8mys1y2qMZj2ckT7PUVsdBpSI (accessed 18 march 2023)

[53] En.wikipedia. 2023. Acetone. https://en.wikipedia.org/wiki/Acetone (accessed 7 November 2022)

[54] Ebi. 2017. Acetone. https://www.ebi.ac.uk/chebi/searchId.do?chebiId= CHEBI:15347 (accessed 7 November 2022)

[55] Hydroxyethylcellulose (HEC). (n.d.). lotioncrafter. https://lotioncrafter.com/products /hydroxyethylcellulose-hec-1 (accessed 25 January 2023)

[56] Hydroxyethyl Cellulose (HEC, HMHEC) Properties and Applications. (n.d.). poly merdatabase. https://polymerdatabase.com/Polymer%20Brands/HEC.html (accessed 25 January 2023)

[57] Hydroxyethyl cellulose. (n.d.). en.wikipedia. https://en.wikipedia.org/wiki/Hydroxy ethyl_cellulose (accessed 25 January 2023)

[58] Polyethylenglycol. (n.d.). de.wikipedia. https://de.wikipedia.org/wiki/ Polyethylengly col (accessed 7 November 2022)

[59] GLYCOLS PEG1500. (n.d.). gravitychemicals. https://www.gravitychemicals.Com /product/india-glycols-ltd/peg-1500-india-glycols/#woocommerce-tabs (accessed 7 November 2022)

[60] Hydroxyethyl cellulose. (n.d.). en.wikipedia. https://en.wikipedia.org/wiki/ Hydroxyethyl_ cellulose (accessed 25 January 2023)

[61] Hydroxyethylcellulose (HEC). (n.d.). lotioncrafter. https://lotioncrafter.com/ products/ hydroxyethylcellulose-hec-1 (accessed 25 January 2023)

[62] PEG 1500 (Polyethylene Glycol 1500). (n.d). atamankimya. https://atamankimya.com /sayfalar.asp?LanguageID=2&cid=3&id=2565&id2=10250 (accessed 7 November 2022)

[63] Acrylic Acid, Ammonium Salt Polymer. (n.d.). guidechem. https://www.guide chem.com/structuresearch/search.html?dictid=AC63D1E6D9420255 (accessed 14 January 2023)

[64] Ammonium polyacrylate. (n.d.) Aapedia. http://www.saapedia.org/en/saa/?type =detail&id=823 (accessed 14 January 2023)

[65] Watsa K, Weerapong B, and Patcharawadee P. 2014. Enhancement forward osmosis (FO) process by using Polyelectrolytes as a draw solution for printing wastewater treatment. Bangkok. https://kb.psu.ac.th/psukb/bitstream/2016/12676/ 1/424488.1.pdf

[66] Ammonium Polyacrylate. (n.d.). products. https://www.products.pcc.eu/th/inci-26/ammonium-polyacrylate/ (accessed 14 January 2023)

[67] Process for producing polyacrylic acid salt granules easily soluble in water. (n.d.). patents google. https://patents.google.com/patent/US4386120A/en (accessed 14 January 2023)

[68] Insoluble polyacrylic acid salts and method of preparing the same. (n.d.). patents.google. https://patents.google.com/patent/US3090736A/en (accessed 14 January 2023)

[69] Watsa K, Weerapong B, and Patcharawadee P. 2014. Enhancement forward osmosis (FO) process by using Polyelectrolytes as a draw solution for printing wastewater treatment. Bangkok. https://kb.psu.ac.th/psukb/bitstream/2016/12676/ 1/424488.1.pdf

[70] Insoluble polyacrylic acid salts and method of preparing the same. (n.d.). patents.google. https://patents.google.com/patent/US3090736A/en (accessed 14 January 2023)

[71] Polyethylene glycol 1500. (n.d.). sigmaaldrich. https://www.sigmaaldrich. com/TH/en/product/mm/807489 (accessed 7 November 2022)

[72] Janani M, Ramalingam C, Sivaramakrishnan S. 2020. Sulfated polysaccharides and its commercial applications in food Industries. Food Science and Technology 58 (7): 2453-2466.

[73] Agaropectin. (n.d.). sciencedirect. https://www.sciencedirect.com/topics/ chemistry/agaropectin (accessed 4 October 2022)

[74] Agars. (n.d.). oxoid. http://www.oxoid.com/UK/blue/techsupport/its.asp?itsp=faq&cat=toxin+detection&faq=tsfaq014&c=UK&lang=EN&print=Y (accessed 4 October 2022)

[75] Jaleh V, Mohammad Reza Z, Mohsen M, and Jaafar B. 2014. Preparation, Optimization, and Screening of the Effect of Processing Variables on Agar Nanospheres Loaded with Bupropion HCl by a D-Optimal Design. *BioMed Research International* 2015 (4):1-13.

[76] What Is AGAR-AGAR?. (n.d.). Agargel. https://agargel.com.br/en/agar-agar/ (accessed 4 October 2022)

[77] Aungsima S. 2021. The Effect of sugar substitutes on Physicochemical and Microstructure of Reduces Sugar Coconut Milk Jelly. Silpakorn University, Nakhon Pathom.

[78] Chemical and Physical Properties of Agar in Cooking. (n.d.). scienceofcooking. https://www.scienceofcooking.com/chemical_physical_properties_agar.htm (accessed 4 October 2022)

[79] Mahmoud N. 2021. *Biopolymer-Based Metal Nanoparticle Chemistry for Sustainable Applications.* Elsevier.

[80] Bitesizebio. 2008. Agarose Gels Do Not Polymerise. https://bitesizebio.com/10248/agarose-gels-do-not-polymerise/ (accessed 4 October 2022)

[81] Chemical and Physical Properties of Agar in Cooking. (n.d.). scienceofcooking. https://www.scienceofcooking.com/chemical_physical_properties_agar.htm (accessed 4 October 2022)

[82] Rafael Armisen and Fernando G. (n.d.). Chapter 1 - Production, Properties and used of agar. Fao. https://www.fao.org/3/x5822e/x5822e03.htm (accessed 4 October 2022)

[83] What Is AGAR-AGAR?. (n.d.). Agargel. https://agargel.com.br/en/agar-agar/ (accessed 4 October 2022)

[84] Viscoelasticity and dynamic mechanical testing. (n.d.). tainstruments. https://www.tainstruments.com/pdf/literature/AAN004_Viscoelasticity_and_DMA.pdf (accessed 25 November 2022)

[85] Glycosidic Bond Formation | Glycosidic Linakage Overview. (n.d.). study.com. https://study.com/learn/lesson/glycosidic-bond.html (accessed 20 February 2023)

[86] Paolo Z. Roberto Fernandez-L. and Enrico S. 2016. Agarose and Its Derivatives as Supports for Enzyme Immobilization. *Molecules* 21 (11): 1577.

[87] Rafael Kenji N., Ellen R, Mara Gabriela Novy Q, Dachamir H, Kurosch R, and Michaela W. 2021. Effect of MgO on the microstructure and properties of mullite membranes made by phase inversion tape casting. Asian Ceramic Societies 9 (3): 1228-1238.

[88] Andrea S, Riccardo L, Matteo D'Este, Susanna P, David E, and Jos M. 2020. Printability and Shape Fidelity of Bioinks in 3D Bioprinting. *Chemical Reviews*.

[89] Technical specifications of ceramic membranes. (n.d.). .lenntech. https://www.lenntech.com/ceramic-membranes-features.htm (accessed 7 March 2023)

[90] Technical specifications of ceramic membranes. (n.d.). .lenntech. https://www.lenntech.com/ceramic-membranes-features.htm#ixzz7a2DXt4vd (accessed 7 March 2023)

[91] Zhenyu Y, Chengyi C, Diwei Z, Siwei M, Jianjun G, Yuchuan C, Gaojie X, Zhixiang L, Aihua S. 2021. Study on 3D-Direct Ink Writing based on adding silica submicron-particles to improve the rheological properties of alumina ceramic ink. Materialstoday Communications (28): 102534.

[92] What Are The Requirements For Ceramic Membrane Operation?. (n.d.). Jiuwu membrane. https://www.jiuwumembrane.com/what-are-the-requirements-for-ceramic-membrane-operation.html (accessed 7 March 2023)

[93] Rozita M, Toraj M. 2020. Chapter 5 - Nanostructured membranes for water treatments. *Nanotechnology in the Beverage Industry*: 129-150.

[93] Shuangjun H, Chunsheng Y, Huoping Z, and Zitian F. 2019. Additive Manufacturing of Thin Alumina Ceramic Cores Using Binder-Jetting. *Additive Manufacturing* 29 (12):100802.

[94] What is Additive Manufacturing? Definition, Types and Processes. (n.d.). twi-global. https://www.twi-global.com/technical-knowledge/faqs/what-is-additive-manufacturing (accessed 24 February 2023)

[95] Additive Manufacturing. (n.d.). sciencedirect. https://www.sciencedirect.com/ topics/ engineering/additive-manufacturing (accessed 24 February 2023)

[96] Hydroxyethyl Cellulose. (n.d.). sciencedirect . https://www.sciencedirect.com/topics/ biochemistry-genetics-and-molecular-biology/hydroxyethyl-cellulose (accessed 25 January 2023)

[97] Viscoelasticity and dynamic mechanical testing. (n.d.). tainstruments. https://www.tainstruments.com/pdf/literature/AAN004_Viscoelasticity_and_DMA.pdf (accessed 25 November 2022)

[98] K. Fu, Y. Wang, C. Yan, Y. Yao, Y. Chen, J. Dai, S. Lacey, Y. Wang, J. Wan, T. Li, Z. Wang, Y. Xu and L. Hu: Graphene Oxide-Based Electrode Inks for 3D-Printed LithiumIon Batteries (WILEY-VCH Verlag GmbH & Co. KGaA, Weinheim, Germany 2016).

[99] Z. Chen, Z. Li, J. Li, C. Liu, C. Lao, Y. Fu, C. Liu, Y. Li, P. Wang and Y. He: 3D printing of ceramics: A review (Elsevier, 2019).

[100] L. Rueschhoff, W. Costakis, M. Michie, J. Youngblood, and R. Trice: Additive Manufacturing of Dense Ceramic Parts via Direct Ink Writing of Aqueous Alumina Suspensions (International Journal of Applied Ceramic Technology, 2016).

[101] E. Feilden, E. García-T. Blanca, F. Giuliani, E. Saiz and L. Vandeperre: Robocasting of structural ceramic parts with hydrogel inks (Elsevier, 2016).

[102] L. Yang, X. Zeng and Y. Zhang: 3D printing of alumina ceramic parts by heat-induced solidification with carrageenan (Elsevier, 2019).

[103] H.P. Hsieh, in: Inorganic Membranes for Separation and Reaction. Elsevier, Alcoa Technical Center, Alcoa Center, PA, USA (1996), in press.

[104] D. Saha and S. Bhattacharya: Hydrocolloids as thickening and gelling agents in food: a critical review (Springer, 2010).

[105] E. D. Giuseppe, in: Analogue Materials in Experimental Tectonics. Elsevier, CEMEFCentre de mise en forme des matériaux, Sophia Antipolis Cedex, France (2018), in press.

[106] M. Lahaye: Developments on gelling algal galactans, their structure and physicochemistry (Kluwer Academic Publishers, Netherlands 2001).

[107] Information on https://en.wikipedia.org/wiki/Hydroxyethyl cellulose.

[108] B. R. Thompson, T. S. Horozov, S. D. Stoyanov and V. N. Paunov: An ultra melt-resistant hydrogel from food grade carbohydrates (Royal Society of Chemistry Publishing, London UK 2017).

[109] A. J Millán, R. Moreno and M. I. Nieto: Thermogelling polysaccharides for aqueous gelcasting—part I: a comparative study of gelling additives (Elsevier, 2002).

[110] Y. Yang, S. Shimai, and S. Wang: Room-temperature gelcasting of alumina with a watersoluble copolymer (Materials Research Society, 2013).

[111] What are the types of 3D printers and what can they do?. (n.d.). hubs. https://www.hubs.com/knowledge-base/types-of-3d-printing/ (accessed 25 January 2023)

# APPENDICES

# Appendix A: The paper was published

*Materials Science Forum*
*ISSN: 1662-9752, Vol. 1090, pp 67-73*

*Submitted: 2023-02-02*
*Accepted: 2023-03-11*
*Online: 2023-05-31*

## Direct Ink Writing of Tubular $Al_2O_3$ Membrane Support Using Agar-Based Ink in 3D-Printing

Kotchaphan Chaisong[1,4,a,*], Anukorn Phuruangrat[1,b], Thanyagamon Kanesom[2,c], Kanit Soongprasit[3,d] and Kowit Lertwittayanon[1,4,e]

[1]Materials Science Program, Division of Physical Science, Faculty of Science, Prince of Songkla University, 90112, Thailand

[2]Physics Program, Division of Physical Science, Faculty of Science, Prince of Songkla University, 90112, Thailand

[3]National Metal and Materials Technology Center (MTEC), Thailand Science Park, National Science and Technology Development Agency (NSTDA), Pathumthani, 12120, Thailand

[4]Center of Excellent in Membrane Science and Technology (CoE-MST), Prince of Songkla University, 90112, Thailand

[a]fern_chaisong@hotmail.com, [b]anukorn.p@psu.ac.th, [c]kanesom.thanyagamon@gmail.com, [d]kanit.soo@mtec.or.th, [e]kowit.l@psu.ac.th

**Keywords:** agar, $Al_2O_3$ membrane, additive manufacturing, direct ink writing, 3D printing.

**Abstract.** Direct ink writing was used for 3D printing of tubular $Al_2O_3$ membrane support. Agar-based ink mixtures were prepared as a paste with a proper viscoelastic behavior in achieving printing. Using agar only for mixing with $Al_2O_3$ slurry in preparing the ink mixtures showed the flow behavior resulting in failure to print the $Al_2O_3$ tube due to too low viscosity of the ink mixture—100 Pa at 40°C. However, the introduction of Hydroxyethyl cellulose (HEC) as thickener and Polyethylene glycol 1500 (PEG 1500) as lubricant helped improve the behavior of the ink mixtures to be more proper paste for printing. The amounts of HEC were varied from 0 to 2wt% of solid loading. At 2wt% HEC, the ink mixture was able to be printed highest, compared to the other ink mixtures. However, the 2wt% HEC-using ink mixtures possessed the highest sintering shrinkage at 12%, while its relative density was highest at 70%. The results indicated that it was possible to print the alumina membrane tube if its fidelity was improved further.

### Introduction

Direct ink writing (DIW) was a slurry-based 3D printing widely used for fabricating complex-shaped ceramics. Its popular use originated from the advantages of simplicity, inexpensive cost, and capability to print both monolithic and composite [1]. DIW was a technique relying on extrusion of non-newtonian viscous slurry or paste and layering up with no deformation of initial shape [2]. Properties in terms of rheology were determined by the ratio of binder to ceramic particles. Therefore, the composition of paste was essential for the quality of printed ceramics.

Rueschhoff et. al. [3] reported that 53 – 56 vol% solid loadings were optimum for printing $Al_2O_3$ sample using nozzle with 1.25 mm in diameter. It was indicated that at 51 vol% solid loading its yield stress was insufficient to support the weight in higher layers. On the other hand, uneven deposited layer height was observed for 58 vol% solid loading. The hydrogel-based DIW was examined by Feiden and co-workers [4]. Pluronic F-127 was used in their ink mixtures and thereby approximate the rheological properties by Herschel and Bulkley's model. It was found that storage modulus of hydrogel was comparable to that of colloidal suspension; however, it suffered from lower ceramic volume fraction. The hydrogel showed the yield stress higher than the colloidal suspension. Yang et. al. [5] used carrageenan as an additive in the heat induced DIW ink. The ink containing carrageenan exhibited pseudoplastic model of fluid for which was desirable for DIW. Using carrageenan in the ink mixture helped swelling and absorbing water reducing free water in slurry and thus increasing the solid loading.

In this work, $Al_2O_3$ membrane support with tubular shape was 3D printed by DIW. Using 3D printer for shaping the $Al_2O_3$ membrane support was to find an alternative displacing an expensive extruder for which was a common machine for shaping ceramic with tubular shape [6]. Moreover, 3D printing might open a window of ceramic membrane with further complicated shapes. Therefore, it was worth adapting DIW for shaping the ceramic membrane support. To shape using the DIW technique, agar was selected as a thickener of ink mixtures and a gelling agent after injecting out of nozzle of the printer [7]. Consequently, the concentrations of agar in the form of solution were examined for the possibility of printability. After printing the ink mixtures, one of the ink mixtures was used for improving further its rheological properties. In the improvement in terms of rheology, additives were introduced into the agar-based ink mixtures such as Hydroxyethyl cellulose (HEC) as thickener and Polyethylene glycol 1500 (PEG 1500) as lubricant [8]. The additives-modified ink mixtures were 3D printed and characterized for observing microstructure and shrinkage.

**Materials and Method**

**Raw Materials**. α-$Al_2O_3$ powder (TM-5D, Taimei Co.,Ltd., Japan) with average particle size of 0.2 μm was used for fabricating the tubular $Al_2O_3$ membrane support. Magnesia (MgO) nanopowder (Alfa Aesar) was used as a sintering aid. Ammonium salt of polyacrylic acid (Dispex AA 4040, BASF) was employed as a dispersant. Agar powder was added into the ink in the form of agar solution for functioning as a thickener of the printing ink and then gel formation after being injected from nozzle of printer. To further increase the viscosity of ink, Hydroxyethyl cellulose (HEC, Ashland Industries, Netherlands) was used as a thickener and stabilizer. Polyethylene glycol 1500 (PEG 1500, Loba Chemie PVT. Ltd) was used as a lubricant. Acetone (99.8% purity) was added into the prepared ink to form rapidly dried filament of ink relying on the evaporation of acetone at room temperature. Reverse osmosis (R/O) water was used in preparing all the printing ink.

**Ink Preparation**. The $Al_2O_3$ slurry with solid loading of 80wt% was prepared by ball milling in HDPE bottle for 2 h to ensure the full dispersion of $Al_2O_3$ powder. MgO was used at 0.03wt% of the solid loading and Dispex was added to the slurry at 1wt% of the solid loading. After ball milling, the $Al_2O_3$ slurry was kept warm in an ultrasonic bath at 60ºC. For preparing agar solution, the agar powder was mixed with RO water and then stirred using magnetic bar at the same time as boiling on a hot plate until a clear yellow solution was observed. The concentration of agar solution was fixed at 2wt%. However, the addition of the agar solution to the $Al_2O_3$ slurry was varied at different concentration of 1, 2, 3 and 4wt%. However, real agar content was fixed at 2wt% of solid loading. All the mixtures of agar solution and $Al_2O_3$ slurry were measured by a rheometer (HR-2, TA Instruments, USA) to examine their viscoelastic properties—storage modulus (G') and viscosity. The prepared agar-based ink was 3-D printed into a cup for preliminary examination at 40ºC before the agar transformation into gel completely. A temperature in printing was selected from the viscosity result. Thereafter, one of the ink mixtures was selected for further adding HEC to increase the viscosity of ink for being printable. Since the viscosity of agar-adding ink was too low, it needed to add the thickener—HEC. HEC was selected as the thickener for the agar-based ink since it possessed the same negative charge as agar. Thereby, agar and HEC were able to be well dispersed, regardless of their proportion. The molecular structures of agar and HEC were shown in Fig. 1a) and b), respectively. HEC was varied at 0, 1 and 2wt% of the solid loading using mechanical stirrer for obtaining the homogeneous ink. In addition to the HEC addition, PEG 1500 was added to the prepared ink at the fixed proportion of 10wt% of solid loading. In the preparation of ink modified with the additives, the agar powder was first boiled until the clear solution was obtained. Subsequently, HEC flakes and PEG 1500 were added into the clear agar solution, respectively, prior to mixing mechanically with the prepared warm $Al_2O_3$ slurry at 60ºC in the ultrasonic bath. Finally, the mixtures of ink were cooled down to RT before the 3-D printing of $Al_2O_3$ tube. It meant that the printing temperature needed no consideration in the case of the additives-modified ink. The prepared ink showed the characteristic like a paste as shown in Fig. 1c).

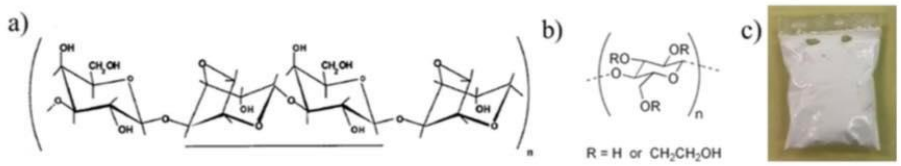


Figure 1. Molecular structures of a) agar [9] and b) hydroxyethyl cellulose [10], including c) photograph example of agar-based ink modified with the additives.

**Printing of Agar-Based Ink into $Al_2O_3$ Tube.** The prepared agar-based ink was 3-D printed into the tubular shape by Eazao zero printer, China. The main parameters in 3-D printing set by Cura program included: 1) 1-mm layer height, 2) 1 mm/s print speed, 3) 1.5 mm z hop height. The diameter of nozzle was 1.5 mm. The prepared ink was poured into a syringe barrel equipped with the 3-D printer. The direct ink writing was conducted by extrusion through a screw and then nozzle driven by a stepping motor. The ink paste was driven through the nozzle with 1.5 mm in diameter. The dimension of tubular $Al_2O_3$ was 3-cm outer diameter and 0.5-cm thickness. After 3-D printed, the tube was dried in air for 24 h and then sintered at 1300ºC for 1 h.

**Characterization**. The rheological behavior of agar-based ink mixtures at concentration 1, 2, 3 and 4wt% was analyzed by the rheometer. In ramp mode, the viscosity was tested at shear rates of 1–100 $s^{-1}$. In oscillation mode, the storage modulus (G') was measured at frequency of 1 Hz and ramp of 0.5ºC/s. The diameter of measuring cup and the test gap was 15 mm and 1000 μm, respectively. The microstructure of sample was observed by SEM (JSM 5800LV, JEOL, Netherlands) at 20 kV. The sintered samples were cut with SiC cutting wheel. The cut samples were dried in an oven at 110ºC for 24 h. The samples were gold coated using 2-times sputtering for 60s each.

## Results and Discussion

The rheological behavior of the printing ink including the storage modulus and the viscosity was shown in Fig. 2a) and b), respectively. It clearly showed in Fig.2a) that the ink prepared from 1wt% concentration of agar solution had the behavior of storage modulus different from that of other ink mixtures. The storage modulus of ink at 1wt% concentration was markedly low from cooling at 70 down to 40ºC. The unusual behavior was attributed the presence of too much water in this ink mixture. It was also observed in its experiment that there was the precipitation of $Al_2O_3$ particles rapidly in the preparation step being the behavior of ink unsuitable for printing. It was found that there was truly 31-wt% $Al_2O_3$ loading in the final prepared ink. The $Al_2O_3$ loading was equal 10 vol% of the prepared ink mixture.

In contrast to the other ink mixtures, the degree of storage modulus was steady from 70 to 45ºC and then increased sharply when the temperature further decreased from 45ºC. The temperature at 50ºC was selected for 3D printing in this work since it was a proper temperature for the unchanged storage modulus and being above the further markedly increasing temperature of storage modulus at only 5ºC. In other words, it was the proper temperature facilitating the extrusion of ink through the nozzle and the rapid transformation into gel of agar molecules able to keep the shape of filament of ink—good fidelity. From all the ink mixtures, the concentration of agar solution at 4wt% indicated the highest storage modulus between 70 and 45ºC. In comparison to the storage modulus of solution containing agar only—agar solution, it was found that the tendency of the storage modulus of agar-based ink mixtures clearly differed from those of agar solution in the work of Thompson et. al. [11]. The storage modulus of agar solution was rapidly developed from 85 down to 55ºC. However, that of ink mixtures increased from 45 to 30ºC. It implied that the presence of $Al_2O_3$ particles in the ink mixtures delayed the development of gelation of agar molecules. It was noticed that the degrees of storage modulus for using the same 2wt% concentration at 40ºC were approximately 30000 and 100

Pa for the pure agar solution and ink mixture, respectively. The huge difference of storage modulus indicated the possibility of poor fidelity of the printed tube due to the rather low storage modulus.

Fig. 2b) showed the viscosity behavior of all the prepared ink mixtures. The degree of viscosity clearly increased when the concentration of agar solution increased from 1 to 4wt%. Especially for 4wt% concentration, the viscosity of ink mixture significantly increased in comparison to the other ink mixtures. The result of viscosity suggested that the ink mixture prepared from 4wt% concentration of agar solution created paste-like characteristic suitable for further printing the tube. From Fig. 2a) and 2b), it was obvious that the ink mixture prepared from 4wt% concentration of agar solution possessed the degrees of storage modulus and viscosity much more than that prepared from the other concentration. In taking account of only the viscosity of ink mixtures, the values of their viscosity were in the range between 0.2 and 1.5 Pa·s, corresponding with the viscosity of solution containing only agar reported by Millán et. al. [12].

From Fig. 2a) and b), it was obvious that the trend of the storage modulus and viscosity was able to be divided into 2 groups: 1) at ≤ 3wt% concentration, and 2) at > 4wt% concentration. When the concentration was ≤ 3wt%, their degrees of storage modulus were considerably low, i.e. no more than 10 Pa in the range of temperature between 70 down to 45°C. The storage modulus sharply increased when the temperature reached 45°C which were between 1000 and 10000 Pa. On the contrary, when the concentration was > 4wt%, the storage modulus was relatively high about 100 Pa in that range from70 to 45°C. However, the storage modulus turned out to be relatively a few increased from 200 to 3000 Pa. The tendencies of storage modulus implied the direct relationship between the used concentration of agar solution and the behaviors of storage modulus. It indicated that when there were a few amounts of agar molecules compared with $Al_2O_3$ particles in the ink mixtures, the behaviors of storage modulus were governed by the $Al_2O_3$ particles being the property of solid, or, more precisely, elastic property due to the presence of $Al_2O_3$ particles. While the ink mixtures were transforming to gel phase, the behaviors of elastic solid were prominent. For at 4wt% concentration, the behavior of storage modulus was affected by the increasing amounts of agar molecules in the ink mixture. It was noticeable that the storage modulus did not sharply increase since the presence of agar gel might be sufficient to determine the elastic property of ink mixture. For the tendency of viscosity, it showed the behaviors able to be divided into 2 groups in the same way as that of storage modulus. The results of viscosity were attributed to the increasing amounts of agar as well.

Fig. 3 displayed the filament of printed ink mixture prepared from the concentration of agar solution at 4wt%. Although the ink mixture was extruded through the nozzle, its fidelity was quite poor. The shape of ink filament extruded out of the nozzle changed owing to the flow of filament and finally the struggle with up layering. For the other ink mixtures prepared from the concentration of agar solution less than 4wt%, their fidelity was poorer than the ink mixture using 4wt% concentration. The preliminary printing into the cup of the agar-based ink mixtures pointed out that the viscosity degree was not enough for attaining the high fidelity. Therefore, the thickener—HEC—was selected for improving the viscosity of ink being like a paste for printing.

Fig. 4a) – c) displayed the printed tubes introducing HEC as the thickener in the ink mixtures at the different amounts from 0 to 2wt%. It should be remined that this variation of HEC in the ink mixtures came alongside the fixed amounts of PEG 1500 at 10wt% of solid loading. It clearly showed that the fidelity of all printed tubes was enhanced with the increasing amounts of HEC. The enhanced fidelity was closely related to the increase in viscosity due to the increasing amounts of HEC as the thickener. It was noticable that the printing ink mixtures were able to be printed at the higher levels when the added amounts of HEC increased from 0 to 2wt%. It was interesting that the ink mixtures modified by HEC and PEG 1500 were able to print at room temperature. As a result, the compositions of ink consisting of agar, HEC and PEG 1500 offerred the capability to print at the room temperatre. It was found that a copolymer— Isobam, was able to be used as dispersant and gelling agent of $Al_2O_3$ gelcasting at the room temperature [13]. Conseqently, Using agar, HEC and PEG 1500 together might help the printability successful at the room temperature.

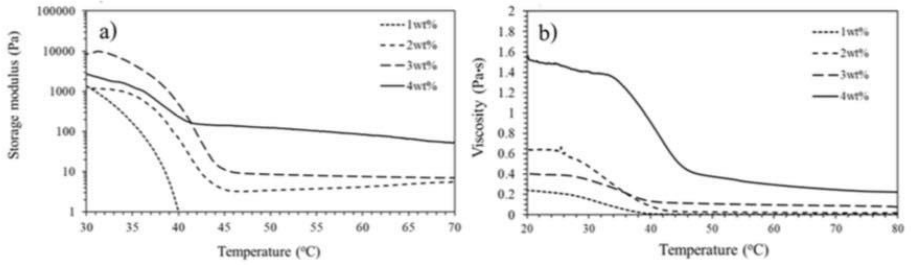


Figure 2. a) storage modulus and b) viscosity of ink prepared from different concentration of agar solution at 1, 2, 3 and 4wt%.

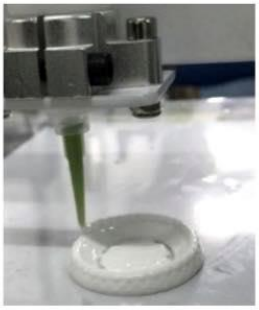

Figure 3. Photographs of printing ink sample prepared from 4wt% concentration of agar solution.

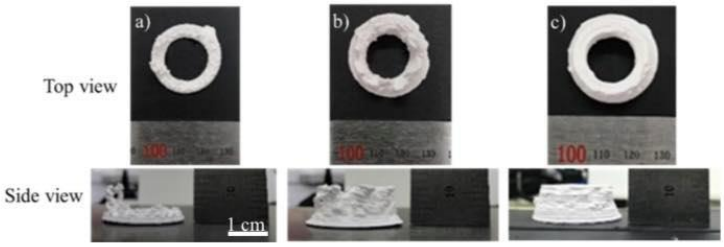


Figure 4. Printed samples of $Al_2O_3$ tubes with the HEC content at a) 0wt%, b) 1wt%, and c) 2wt%; while the amounts of agar and PEG 1500 were fixed.

Table 1 showed the relative density and sintering shrinkage of the printed tube after sintering at 1300°C. When the HEC content increased from 0 to 2wt%, the relative density increased from 58 to 70%. However, the tendency of relative density was different from that of sintering shrinkage. In other words, the sintering shrinkage increased from 6.3 to 12.1% with increasing the HEC content. The results suggested that adding 2wt% HEC caused the increasing shrinkage during sintering leading to the increasing relative density. Thus, it might imply that the amount of HEC at 2wt% enhanced the compaction of $Al_2O_3$ particles in the ink mixtures leading to the higher shrinkage and thereby the higher relative density.

Fig. 5 indicated the SEM images of the printed tubes after sintering. It showed that the grain sizes of $Al_2O_3$ were larger with increasing the HEC content, especially at 2wt% HEC. The increasing grain sizes were in agreement with the results of relative density.

Table 1. Physical properties of printed tubes prepared from the different amounts of HEC.

| Composition | Bulk density ($g/cm^3$) | Relative density (%) | Sintering shrinkage (%) |
|---|---|---|---|
| 0wt% HEC | 2.3 | 58 | 6.3 |
| 1wt% HEC | 2.3 | 58 | 5.9 |
| 2wt% HEC | 2.8 | 70 | 12.1 |

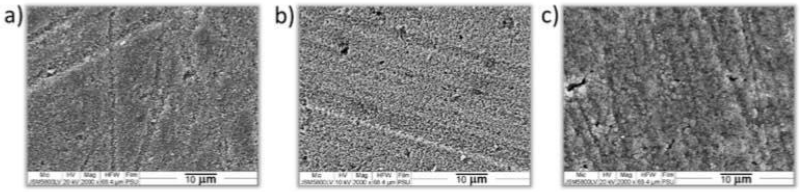


Figure 5. SEM images of sintered $Al_2O_3$ tubes with the HEC content at a) 0wt%, b) 1wt%, and c) 2wt%.

**Conclusion**

The $Al_2O_3$ tubes were shaped by DIW for using as membrane support. The agar-based ink mixtures using agar only was unable to be printed due to the too low viscosity. To increase the viscosity, the thickener and lubricant being HEC and PEG 1500, respectively, were introduced into the agar-based ink mixtures. The HEC addition at 2wt% provided the best printability and highest relative density. It should be noted that the fidelity of printed tubes must be enhanced further to form the tubes with the increasing height. The compositions consisting of agar, HEC and PEG 1500 were enable the printing at the room temperature.

**Acknowledgement**

This research work was financially supported by Thailand Graduate Institute of Science and Technology (TGIST) (grantee code: TG-MT-PSU-63-057M)

**References**

[1] K. Fu, Y. Wang, C. Yan, Y. Yao, Y. Chen, J. Dai, S. Lacey, Y. Wang, J. Wan, T. Li, Z. Wang, Y. Xu and L. Hu: *Graphene Oxide-Based Electrode Inks for 3D-Printed Lithium-Ion Batteries* (WILEY-VCH Verlag GmbH & Co. KGaA, Weinheim, Germany 2016).

[2] Z. Chen, Z. Li, J. Li, C. Liu, C. Lao, Y. Fu, C. Liu, Y. Li, P. Wang and Y. He: *3D printing of ceramics: A review* (Elsevier, 2019).

[3] L. Rueschhoff, W. Costakis, M. Michie, J. Youngblood, and R. Trice: *Additive Manufacturing of Dense Ceramic Parts via Direct Ink Writing of Aqueous Alumina Suspensions* (International Journal of Applied Ceramic Technology, 2016).

[4] E. Feilden, E. García-T. Blanca, F. Giuliani, E. Saiz and L. Vandeperre: *Robocasting of structural ceramic parts with hydrogel inks* (Elsevier, 2016).

[5] L. Yang, X. Zeng and Y. Zhang: *3D printing of alumina ceramic parts by heat-induced solidification with carrageenan* (Elsevier, 2019).

[6] H.P. Hsieh, in: *Inorganic Membranes for Separation and Reaction.* Elsevier, Alcoa Technical Center, Alcoa Center, PA, USA (1996), in press.

[7] D. Saha and S. Bhattacharya: *Hydrocolloids as thickening and gelling agents in food: a critical review* (Springer, 2010).

[8] E.D. Giuseppe, in: *Analogue Materials in Experimental Tectonics*. Elsevier, CEMEF-Centre de mise en forme des matériaux, Sophia Antipolis Cedex, France (2018), in press.

[9] M. Lahaye: *Developments on gelling algal galactans, their structure and physico-chemistry* (Kluwer Academic Publishers, Netherlands 2001).

[10] Information on https://en.wikipedia.org/wiki/Hydroxyethyl cellulose.

[11] B.R. Thompson, T. . Horozov, S.D. Stoyanov and V.N. Paunov: *An ultra melt-resistant hydrogel from food grade carbohydrates* (Royal Society of Chemistry Publishing, London UK 2017).

[12] A.J Millán, R. Moreno and M. I. Nieto: *Thermogelling polysaccharides for aqueous gelcasting—part I: a comparative study of gelling additives* (Elsevier, 2002).

[13] Y. Yang, S. Shimai, and S. Wang: *Room-temperature gelcasting of alumina with a water-soluble copolymer* (Materials Research Society, 2013).

## Appendix B: Raw data of experimental results

**Part I:** Physical properties

| Agar solution composition fixed 10wt%PEG | $W_1$ fired weight (1300ºC) | $W_2$ suspended weight (g) | $W_3$ saturated weight (g) | V Volume ($w_3$-$w_2$) | $\rho_A$ Apparent density (g/cm$^3$) | $\rho_B$ Bulk density (g/cm$^3$) | Firing width (mm) | Fired width (mm) | %FS = %firing shrinkage of width | Firing height (mm) | Fired height (mm) | %FS = %firing shrinkage of height | $V_{op}$ Volume of open porosity ($w_3$-$w_1$) | $\%P_A$ = Apparent porosity | $\%A_W$ = water absorption |
|---|---|---|---|---|---|---|---|---|---|---|---|---|---|---|---|
| 0acetone/0HEC | 0.8995 | 0.69 | 1.0718 | 0.3818 | 4.2935 | 2.3559 | 30 | 29 | 3.3333 | 14 | 13 | 7.1428 | 0.1723 | 45.1283 | 19.1550 |
| 0acetone/1HEC | 2.6518 | 2.01 | 3.0648 | 1.0548 | 4.1318 | 2.5140 | 34 | 32 | 5.8823 | 13 | 12 | 7.6923 | 0.413 | 39.1543 | 15.5743 |
| 0acetone/2HEC | 4.9158 | 3.63 | 5.4077 | 1.7777 | 3.8231 | 2.7652 | 33 | 29 | 12.1212 | 16 | 12 | 25 | 0.4919 | 27.6705 | 10.0065 |
| 10acetone/2HEC | 3.8296 | 2.87 | 4.3359 | 1.4659 | 3.9908 | 2.6124 | 31 | 28 | 9.6774 | 13 | 11 | 15.3846 | 0.5063 | 34.5385 | 13.220 |
| 20acetone/2HEC | 3.072 | 2.31 | 3.5309 | 1.2209 | 4.0314 | 2.5161 | 31 | 29 | 6.4516 | 13.5 | 12 | 11.1111 | 0.4589 | 37.5870 | 14.9381 |

**Part II: calculation methods**

Preparation 150 g. of $Al_2O_3$ slurry with 10wt%Acetone, 2%HEC and 10wt%PEG1500 condition

**Solid: water** 80: 20

- $Al_2O_3$ slurry preparing 100 g. — $Al_2O_3$ powder (TM-5D) 80 g.
  $Al_2O_3$ slurry preparing 150 g. — $Al_2O_3$ powder (TM-5D) = (150x80)/100
  ***= solid 120 g.***

- $Al_2O_3$ slurry preparing 100 g. — water 20 g.
  $Al_2O_3$ slurry preparing 150 g. — water = (150x20)/100
  ***= water 30 g.***

**0.03wt% MgO**

- $Al_2O_3$ powder (TM-5D) 100 g. — MgO used 0.03 g.
  $Al_2O_3$ powder (TM-5D) 120 g. — MgO used = (120x0.03)/100
  ***= MgO 0.036 g.***

**Dispex-AA**

- $Al_2O_3$ powder (TM-5D) 100 g. — Dispex AA used 1 g.
  $Al_2O_3$ powder (TM-5D) 120 g. — Dispex AA used = (120x1)/100
  ***= DispexAA 1.2 g.***

**After ball milling for 2 h.**

$Al_2O_3$ slurry weighing 129.66 g.

- $Al_2O_3$ slurry obtaining100 g. — true $Al_2O_3$ powder (TM-5D) 80 g.
  $Al_2O_3$ slurry obtaining129.66 g. — true $Al_2O_3$ powder (TM-5D)
  = (129.66x80)/100 g.
  = True solid 103.728 g.

**Kept warm in ultrasonication at 60 ºC**

**2wt%final agar**

- True solid 100 g. Agar used 2 g.
  True solid 1002.824 g. Agar used = (102.824x2)/100
  = Agar 2.05648 g.
  ***= 50%Agar 1.02824 g.***

**4wt%Agar solution**

- Agar powder 4 g. water 96 g.
  Agar powder 2.05648 g. water = (2.05648x96)/4
  = water 49.35552 g.
  **= 50%*water 24.67776 g.***

Total 50% of 4wt%agar solution 1.02824+24.67776 = 25.706 g.

**10wt% Acetone**

- Agar solution 100 g. Acetone 10 g.
  Agar solution 25.706 g. Acetone = (25.706x10)/100
  ***= Acetone 2.5706 g.***

  Where; $\rho=m/v$

  $v=m/\rho$

  Acetone volume ($V_{acetone}$) = 2.5706/0.79

  ***Acetone preparation = 3.253924051 ml.***

Other solid 98% Agar 2%

**HEC preparing**

- agar powder used 2 g. HEC used 2 g.
  agar powder used 1.02824 g. HEC used = (1.02824x2)/2
  ***= HEC 1.02824 g.***

**- PEG1500 preparing**

- agar powder used 2 g. PEG1500 used 10 g.
  agar powder used 1.02824 g. PEG1500 used = (1.02824x10)/2 g.
  ***= PEG1500 5.1412 g.***

**Part III:** Parameter setting of Cura software for Eazao 3D printer

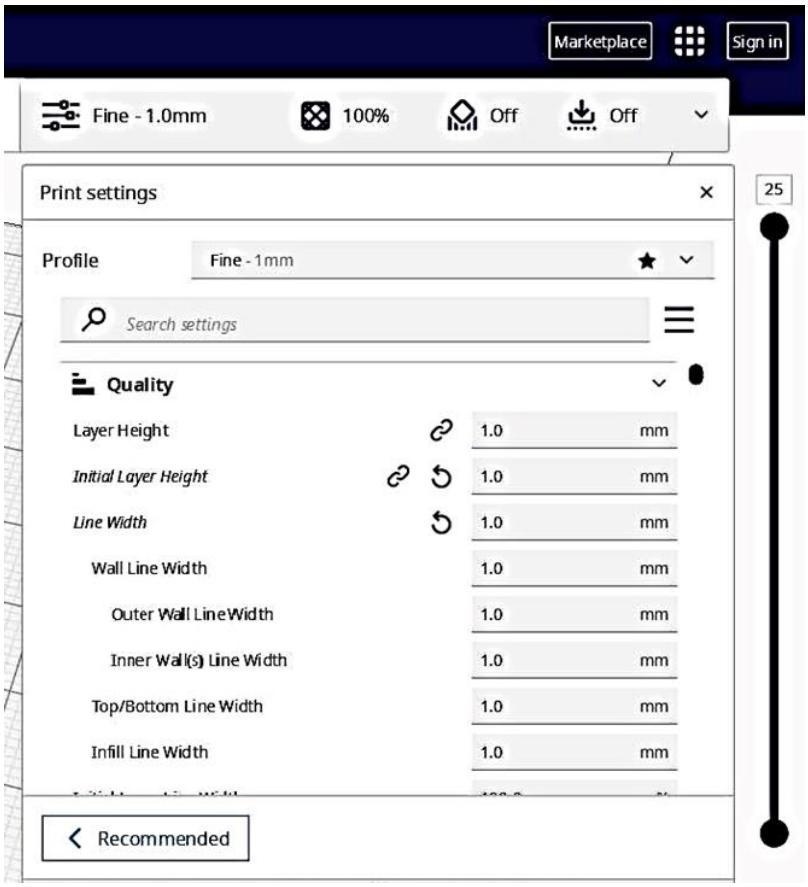


**Quality**

- Layer Height = 1.0 mm
- Initial layer height = 1.0 mm
- Line Width = 1.0 mm
- Wall line width = 1.0 mm

- Outer wall line width = 1.0 mm
- Inner wall(s) line width = 1.0 mm
- Top/Bottom Line width = 1.0 mm
- Infill Line width = 1.0 mm
- Initial layer line width = 100.0%

**Walls**

- Wall Thickness = 2.0 mm
- Wall Line Count = 2
- Wall Transition Length = 1.0 mm
- Wall Distribution Count = 1
- Wall Transitioning Threshold Angle = 10.0 °
- Wall Transitioning Filter Margin = 0.375 mm
- Outer Wall Wipe Distance = 0.75 mm
- Outer Wall Inset = 0.0 mm
- Optimize Wall Printing Order = ☑
- Wall Ordering = Outside to Inside
- Alternate Extra Wall = ☐
- Minimum Wall Line Width = 1.0 mm
- Minimum Even Wall Line Width = 1.0 mm
- Split Middle Line Threshold = 99.0 %
- Minimum Odd Wall Line Width = 1.0 mm
- Add Middle Line Threshold = 99.0 %
- Print Thin Walls = ☐
- Horizontal Expansion = 0.0 mm
- Initial Layer Horizontal Expansion = 0.0 mm
- Hole Horizontal Expansion = 0.0 mm
- Z Seam Alignment = Sharpest Corner
- Seam Corner Preference = Hide Seam

**Top/Bottom**

- Top surface Skin layers = 0
- Top/Bottom Thickness = 1.0 mm
- Top thickness = 1.0 mm
- Top layers = 2
- Bottom thickness = 2.0 mm
- Bottom layers = 2
- Initial Bottom layers = 2
- Top/Bottom pattern = Lines
- Bottom pattern initial layer = Lines
- Monotonic Top/Bottom Order = ☐
- Top/Bottom Line Directions = [ ]
- No Skin in Z gaps = ☐
- Extra skin wall count = 1
- Enable Ironing = ☐
- Skin Overlap Percentage = 5.0%
- Skin Overlap = 0.05 mm
- Skin removal width = 2.0 mm
- Top Skin removal width = 2.0 mm
- Bottom Skin Removal Width = 2.0 mm
- Skin Expand Distance = 2.0 mm
- Top Skin Expand Distance = 2.0 mm
- Bottom Skin Expand Distance = 2.0 mm
- Maximum Skin Angle for Expansion = 90.0 °
- Maximum Skin Width for Expansion = 0.0 mm

**Infill**

- Infill Density = 100.0 %

- Infill Line Distance = 1.0 mm
- Infill Pattern = Lines
- Connect Infill Lines = ☑
- Infill Line Directions = [ ]
- Infill X Offset = 0.0 mm
- Infill Y Offset = 0.0 mm
- Randomize Infill Start = ☐
- Infill Line Multiplier = 1
- Extra Infill Wall Count = 0
- Infill Overlap Percentage = 0.0 mm
- Infill Overlap = 0.0 mm
- Infill Wipe Distance = 0.25 mm
- Infill Layer Thickness = 1.0 mm
- Gradual Infill Steps = 0
- Infill Before Walls = ☑
- Minimum Infill Area = 0.0 $mm^2$
- Infill Support = ☐
- Skin Edge Support Thickness = 0.0 mm
- Skin Edge Support Layers = 0

**Materials**

- Printing temperature = 0.0 $^oC$
- Printing temperature initial layer = 0.0 $^oC$
- Initial Printing temperature = 25.0 $^oC$
- Final Printing temperature = 25.0 $^oC$
- Scaling Factor Shrinkage Compensation = 100.0%
- Horizontal Scaling Factor Shrinkage Compensation = 100.0%
- Vertical Scaling Factor Shrinkage Compensation = 100.0%
- Flow = 100.0%

- Wall Flow = 100.0%
- Outer wall flow = 100.0%
- Inner wall(s) flow = 100.0%
- Top/Bottom Flow = 100.0%
- Infill Flow = 100.0%
- Prime Tower Flow = 100.0%
- Initial Layer Flow = 100.0%

**Speed**

- Print Speed = 1.0 mm/s
- Infill Speed = 1.0 mm/s
- Wall Speed = 1.0 mm/s
- Outer Wall Speed = 5.0 mm/s
- Inner Wall Speed = 5.0 mm/s
- Top/Bottom Speed = 5.0 mm/s
- Travel Speed = 2.0 mm/s
- Initial Layer Speed = 2.0 mm/s
- Initial Layer Print Speed = 1.0 mm/s
- Initial Layer Travel Speed = 1.0 mm/s
- Z Hop Speed = 2.5 mm/s
- Number of Slower Layers = 2
- Flow Equalization Ratio = 100.0 %
- Enable Acceleration Control = ☑
- Enable Jerk Control = ☐

**Travel**

- Enable Retraction = ☑
- Retraction at Layer Change = ☐
- Retraction Distance = 7.0 mm

- Retraction Speed = 25.0 mm/s
- Retraction Retract Speed = 25.0 mm/s
- Retraction Prime Speed = 25.0 mm/s
- Retraction Extra Prime Amount = 0.0 $mm^3$
- Retraction Minimum Travel = 2.0 mm
- Maximum Retraction Count = 100
- Minimum Extrusion Distance Window = 10.0 mm
- Combing Mode = Not in Skin
- Max Comb Distance With No Retract = 0.0 mm
- Avoid Printed Parts When Travelling = ☑
- Avoid Support When Traveling = ☐
- Travel Avoid Distance = 0.625 mm
- Layer Start X = 0.0 mm
- Layer Start Y = 0.0 mm
- Z Hop When Retracted = ☑
- Z Hop Only Over Printed Parts = ☐
- Z Hop Height = 1.5 mm

**Cooling**

- Enable Print Cooling = ☐
- Regular/Maximum Fan Speed Threshold = 10.0 s
- Regular Fan Speed at Height = 1.0 mm
- Regular Fan Speed at Layer = 2
- Minimum Layer Time = 5.0 s
- Minimum Speed = 10.0 mm/s
- Lift Head = ☐

**Support**

- Generate Support = ☐

**Build Plate Adhesion**

- Build Plate Adhesion Type = None

**Dual Extrusion**

**Mesh Fixes**

- Union Overlapping Volumes = ☑
- Remove All Holes = ☐
- Extensive Stitching = ☐
- Keep Disconnected Faces = ☐
- Merged Meshes Overlap = 0.15 mm
- Remove Mesh Intersection = ☐
- Remove Empty First Layers = ☑
- Maximum Resolution = 0.5 mm
- Maximum travel Resolution = 1.0 mm
- Maximum Deviation = 0.025 mm
- Maximum Extrusion Area Deviation = 2000.0 $\mu m^2$

**Specials Modes**

- Print Sequence = All at Once
- Mold = ☐
- Surface Mode = Normal
- Spiralize Outer Contour = ☐
- Relative Extrusion = ☐

**Experimental**

- Slicing Tolerance = Middle
- Infill Travel Optimization = ☐
- Minimum Polygon Circumference = 1.0 mm

- Enable Draft Shield = ☐
- Make Overhang Printable = ☐
- Enable Coasting = ☐
- Fuzzy Skin = ☐
- Flow Rate Compensation Max Extrusion Offset = 0.0 mm
- Flow Rate Compensation Factor = 100.0%
- Wire Printing = ☐
- Use Adaptive Layers = ☐
- Overhanging Wall Angle = 90.0 °
- Overhanging Wall Speed = 100.0%
- Enable Bridge Settings = ☐
- Wipe Nozzle Between Layers = ☐
- Small Hole Max Size = 0.0 mm
- Small Feature Max Length = 0.0 mm
- Small Feature Speed = 50.0%
- Small Feature Initial Layer Speed = 50.0%

# VITAE

**Name** Kotchaphan Chaisong

**Student ID** 6310220028

**Educational Attainment**

| Degree | Name of Institution | Year of Graduation |
|---|---|---|
| Bachelor of Science (B.S.) (Materials Science) | Prince of Songkla University | 2019 |
| Master of Science (M.S.) (Materials Science) | Prince of Songkla University | 2022 |

**Scholarship Awards during Enrolment**

Thailand Graduate Institute of Science and Technology: TGIST

**List of Publication and Proceeding**

- Direct Ink Writing of Tubular $Al_2O_3$ Membrane Support Using Agar-Based Ink in 3D-Printing